Calcareous nannofossil assemblages from El Kef (Tunisia) reveal strong regional and bathymetric controls on Northern Hemisphere recovery patterns following the Cretaceous/Paleogene (K/Pg) mass extinction

Heather L. Jones[1], Lorna Kearns[2], Julio Sepúlveda[3], Christopher M. Lowery[4], Laia Alegret[5], Thomas Westerhold[1], M. Hedi Negra[7], Mark Patzkowsky[8] and Timothy J. Bralower[8]

Corresponding author contact: hjones@marum.de

1. MARUM – Center for Marine Environmental Sciences, University of Bremen, Germany.
2. School of Earth and Environment, University of Leeds, UK.
3. Department of Geological Sciences and Institute of Arctic and Alpine Research (INSTAAR), University of Colorado Boulder, USA.
4. Institute for Geophysics, Jackson School of Geosciences, University of Texas at Austin, USA.
5. Departamento de Ciencias de la Tierra & Instituto Universitario de Ciencias Ambientales, Universidad Zaragoza, Spain
6. Faculty of Sciences of Tunis, University of Tunis El Manar, Tunisia
7. Department of Geosciences, Pennsylvania State University, USA.

Peer review status: This is a non-peer-reviewed preprint submitted to EarthArXiv.

Calcareous nannofossil assemblages from El Kef (Tunisia) reveal strong regional and bathymetric controls on Northern Hemisphere recovery patterns following the Cretaceous/Paleogene (K/Pg) mass extinction

Heather L. Jones, Lorna Kearns, Julio Sepúlveda, Christopher M. Lowery, Laia Alegret, Thomas Westerhold, M. Hedi Negra, Mark Patzkowsky and Timothy J. Bralower

The Cretaceous-Paleogene (K-Pg) mass extinction event ~66.0 million years ago (Ma), led to the elimination of over 75% of species on Earth and drove large-scale ecological reorganization in both the marine and terrestrial realms. In particular, the nearly complete extinction of calcareous nannoplankton-the most dominant phytoplankton group at the end of the Cretaceous- led to a shift in community structure within marine primary producers, which had a profound effect on trophic interactions and the marine carbon cycle. Earliest Paleocene nannoplankton assemblages were comprised of a series of short-lived, opportunistic taxa which we term "boom-bust" successions. Although these high dominance, low diversity assemblages have been observed worldwide, the series of taxa that comprise boom-bust successions, as well as the timing of the switchovers between dominant taxa, are globally heterogeneous. Here, we use the expanded and well-preserved fossil record of calcareous nannoplankton from the Global Stratotype Section and Point (GSSP) for the K-Pg boundary near El Kef, Tunisia to better understand the environmental and ecological conditions that drove boom-bust successions. We then incorporate our data into a statistical meta-analysis that includes nannoplankton records from eight other K-Pg sites in the literature, allowing us to better understand the significance of boom-bust successions in a global context. Our results support earlier findings that indicate that changes in nutrient availability, caused by the gradual restoration of biological pump efficiency following the K-Pg impact, was the main driver of boom-bust successions in the earliest Paleocene. Thus, the series of taxa that comprise boom-bust successions are geographically distinct due to differences in the timing of biological pump recovery, the type of marine environment examined (e.g., neritic vs. pelagic settings), and the influence of regional, or even local, controls on ecology.

Introduction

The bolide impact at the Cretaceous/Paleogene (K/Pg) boundary ca. 66 million years ago (Ma) – which most famously wiped out all non-avian dinosaurs (e.g., Alvarez et al., 1980; Schulte et al., 2010; Chiarenza et al., 2020; Hull et al., 2020; Morgan et al., 2022) – also led to the largest mass extinction in the evolutionary history of calcifying marine plankton (i.e., calcareous nannoplankton and planktonic foraminifera) with >90% species being eliminated (Bown et al., 2004; Fraass et al., 2015; Lowery et al., 2020). In comparison to marine calcifiers, siliceous and organic-walled plankton groups such as diatoms, radiolarians and dinoflagellates, suffered much lower extinction rates, likely due to the ability of some species to form resting cysts (MacRae et al., 1996; Sims et al., 2006; Lowery et al., 2020). Calcareous organisms living at the seafloor (e.g., benthic foraminifera) also did not experience a mass extinction at this time (e.g., Thomas 1990; Culver, 2003; Alegret et al., 2012; Alegret and Thomas, 2013; Alegret et al., 2021;), underscoring that the K/Pg extinction predominantly affected marine calcifers living in the upper water column (Lowery et al., 2020). This high level of extinction selectivity suggests that short-lived, impact-induced surface ocean acidification may have been an important kill mechanism (Henehan et al., 2019; Brugger et al., 2021) with impact-winter and decreased light availability caused by the emission of dust and aerosols also

likely playing a major role (e.g., Vellekoop et al., 2014; Brugger et al., 2021; Junium et al., 2022; Morgan et al., 2022; Senel et al., 2023).

As the most prolific and diverse phytoplankton group at the end of the Cretaceous (Knoll and Follows 2016; Lowery et al., 2020), the near-demise of calcareous nannoplankton at the K/Pg boundary had a major impact on marine ecosystem structure and function. Although primary productivity did not completely cease as originally proposed in the 'Strangelove Ocean' model (Hsü and McKenzie 1985), vacated niche space in the photic zone was filled by alternative phytoplankton groups including dinoflagellates, diatoms and (especially) cyanobacteria (e.g., Vellekoop et al., 2017; Renaudie et al., 2018; Sepúlveda et al., 2019; Bralower et al. 2020; Lowery et al., 2021; Alegret et al., 2022). The reduced capability of these (predominantly) organic phytoplankton groups to form dense marine aggregates – especially when compared to the heavily-mineralized, pre-extinction populations of calcareous nannoplankton and planktic foraminifera – severely reduced the effective ballasting of organic carbon from the surface ocean to the seafloor, thus driving decreased biological pump efficiency (i.e., the 'Living Ocean' Model; D'Hondt et al., 1998; Coxall et al., 2006; Birch et al., 2016; Alvarez et al., 2019). However, the mass extinction's effect on biological pump efficiency and export productivity was geographically- and environmentally-variable, as evidenced by site-to-site differences in the magnitude and sign of benthic foraminiferal accumulation rates and diversity, both of which are strongly influenced by the type and amount of food that is transported from the surface ocean (e.g., Alegret and Thomas 2009;2013; Hull and Norris 2011; Alegret et al., 2012; Sepúlveda et al., 2019; Alegret et al., 2022) This so-called 'Hetereogenous Ocean' (Esmeray-Senlet et al., 2015; Henehan et al., 2019; Alegret et al., 2022) was likely a result of taxonomic differences in spatially- and temporally-restricted cyanobacterial blooms, although this has not been thoroughly documented (Bralower et al., 2020; Alegret et al., 2022).

The recovery patterns of calcareous nannoplankton communities during the early Danian were similarly complex. In the Southern Hemisphere, nannoplankton extinction rates were somewhat lower than in the Northern Hemisphere (Jiang et al., 2010) and earliest Paleocene communities consisted of previously-rare survivor taxa that became regionally incumbent for 300 – 400 kyr post-impact (Jiang et al., 2010; Schueth et al., 2015). In contrast, contemporaneous Northern Hemisphere communities were characterized by successive acmes of newly-evolved taxa, which gave rise to the long-ranging lineages that prevailed throughout much of the Paleogene (Bown, 2005; Jiang et al., 2010; Schueth et al., 2015; Alvarez et al., 2019; Jiang et al., 2019; Jones et al., 2019; Bown et al., 2023). Although early Danian nannoplankton acmes have been observed at all previously-studied Northern Hemisphere sites, the specific taxa that comprised these successions as well as the duration of the acme 'regime' (Alvarez et al., 2019) were geographically variable (Schueth et al., 2015; Jones et al., 2019). For example, the nannoplankton acme regime ended ca. 1.75 Myr post-impact at Ocean Drilling Program (ODP) Site 1209 (Shatsky Rise) in the pelagic (bathyal) sub-equatorial Pacific Ocean (Alvarez et al., 2019), ca. 2 Myr post-impact at International Ocean Discovery Program (IODP) Site U1407 in the mid-latitude pelagic (abyssal) North Atlantic Ocean (Bown et al., 2023) and ca. 2.5 Myr post-impact at hemipelagic IODP – International Continental Scientific Ocean Drilling (ICDP) Site M0077A in the peak-ring of the Chicxulub impact crater (i.e., at "ground-zero" of the mass extinction event; Jones et al., 2019; Lowery et al., 2021; Figure 1).

There is emerging evidence that the eventual termination of the nannoplankton acme regime was intrinsically linked to the recovery of biological pump efficiency (Alvarez et al., 2019), which is

generally estimated using the surface to deep ocean $\delta^{13}C$ gradient measured on planktic foraminiferal tests (or on bulk sediment) and benthic foraminiferal tests respectively (e.g., D' Hondt et al., 1998; Coxall et al., 2006; Birch et al., 2016; 2021). In the peak ring of the Chicxulub impact crater, the switchovers between nannoplankton acmes are directly coincident with changes in the dominant planktic foraminiferal trophic group, indicating a gradual transition from high-nutrient (eutrophic) to low nutrient (oligotrophic) surface ocean environments that is also consistent with increasing biological pump efficiency (Jones et al., 2019; Lowery et al., 2021). If the recovery of biological pump efficiency – which was globally heterogenous as outlined above (e.g., Hull & Norris, 2011; Alegret et al., 2022) – was strongly coupled to calcareous nannoplankton recovery, it is hardly surprising that there is similarly high geographic variability in the duration and signature of the nannoplankton acme regime. Comparison of nannoplankton acme characteristics between different ocean basins and marine environments (i.e., continental shelf → abyssal plain), should therefore reveal region- and environment-specific controls on nannoplankton recovery following the largest mass extinction event in their evolutionary history. However, despite having the potential to provide information regarding how organisms at the bottom of the marine food chain respond to rapid episodes of extreme environmental change – which is also important in a modern climate context – such analyses have rarely been conducted (Jiang et al., 2019).

In order to help facilitate these cross-site and cross-environment comparisons, we present here a high-resolution record of Danian calcareous nannofossil assemblages in sediment cores recovered near the Global Stratotype Section and Point (GSSP) for the basal Danian in El Kef (Tunisia). Our new dataset provides one of the longest and most complete nannofossil records from a K/Pg continental shelf site to date, allowing us to:

(a) fully document the nannoplankton acme regime in a shallow marine depositional setting;

(b) statistically compare the nannoplankton acme regime at El Kef to other Tethyan sites, elucidating the potential importance of local processes in ecosystem recovery; and

(c) statistically compare the nannoplankton acme regimes at El Kef and other Northern Hemisphere sites sampling a range of different ocean basins and marine environments, in an attempt to separate out the environment- and region-specific controls on acme characteristics (e.g., duration of acmes and the specific acme-forming taxa).

Methods

Study site

During the El Kef Coring Project, sediment cores were recovered from five holes located in close proximity to the GSSP outcrop section, ~5 km southwest of the town of El Kef in northwestern Tunisia (Jones et al., 2023). Due to the drilling process, typical features of the K/Pg boundary observed in the El Kef outcrop (e.g., the 2-3 mm iridium lamina) were not captured in the sediment cores. However, the integration of biostratigraphic, geochemical and X-Ray Fluorescence (XRF) data led to precise delineation of the boundary and the construction of a composite section ('splice') (Jones et al., 2023). The resultant preferred age model indicates that the Danian was fully and completely recovered in the El Kef cores, apart from a clear unconformity within planktic foraminiferal biozone P1b that was not previously recognized in outcrop. The Danian sediments at El Kef predominantly consist of gray marls (carbonate-rich mudstones) that are darker in color and less heavily bioturbated below the unconformity (Jones et al., 2023). The entire section was deposited at

a paleolatitude of 25-30°N in the Tethys Ocean (Figure 1), and samples an outer-shelf to upper-slope paleoenvironment with water depths of 200-300 m (e.g., Speijer and Van der Zwaan, 1996; Alegret 2003).

Planktic foraminiferal biostratigraphy

The current preferred age model for the El Kef cores (Jones et al., 2023) is predominantly based on planktic foraminiferal biostratigraphic datums and is considered to be robust for the early Danian (planktic foraminifer biozones P0 through the base of P1b). However, reliability of the age model decreases above this due to challenges in identifying biozone markers within the interval immediately above the unconformity in Hole E, which can be attributed to poor preservation, weathering and reworking. There were also some difficulties in precisely delineating the base of the P2 biozone within Hole C as *Praemurica uncinata* (biozone marker for the base of P2) was very rare and had a somewhat spotty occurrence (Jones et al., 2023). Some of the uncertainty with respect to the delineation of the P2 biozone can also be explained – at least in part – by the fact that generally only the 38 – 63 µm size fraction was examined for the biozone marker taxa, thus excluding the larger specimens that became increasingly more common during the Danian.

To further improve the reliability of our age model, planktic foraminiferal biostratigraphy was conducted on the >75 µm size fraction for 28 samples from El Kef Hole C and 44 samples from El Kef E. The specific purpose of these additional analyses was to better constrain the base of P2 and the timing of the unconformity, whilst ensuring biostratigraphic consistency between different size fractions during the earlier Danian (i.e., biozones P0 through P1b).

Calcareous nannofossil assemblage counts

Using the age model and composite section as a guide, we chose to use samples from Holes E and C, as combined these represent a nearly stratigraphically continuous K/Pg transition from immediately after the mass extinction event to the base of the *Futyania* acme (Hole E), and from the *Futyania* acme to the *Praeprinsius* tenuiculus acme (Hole C). In addition, Hole E has the best nannofossil preservation out of all of the holes, as evidenced by the common occurrence of coccospheres (complete cell coverings of nannoplankton) belonging to all of the ecologically important taxa. Smear slides for nannofossil analyses were made following the standard procedures outlined in Bown (1998) and examined under cross-polarized light at 1600x magnification. Assemblages were analyzed at a 10 cm sampling resolution between ~54.5 m and 61.5 m composite depth, a 10 to 20 cm sampling resolution between ~36.0 m and 54.5 m composite depth, and a sampling resolution of every 60 cm above this. Because the switchovers between K/Pg nannoplankton acmes were geologically rapid events followed by a relatively prolonged interval of quasi-stability, we do not anticipate that the stratigraphic reduction in sampling resolution up-section has drastically altered our results or interpretations.

At least 300 nannofossil specimens were counted along a random transect in each sample and identified to species-level using the taxonomic concepts on Mikrotax and images provided by Dr. Paul Bown at University College London (UCL), to ensure taxonomic consistency between different working groups. Some specimens, including tiny (<2 µm) *Neobiscutum* coccoliths and intermediate, evolutionary morphotypes were difficult to identify to species-level, and thus were only assigned a

genus. Ultimately, our nannoplankton abundance counts resulted in the creation of a large dataset comprising of 201 samples and over 60,000 nannofossil occurrences.

Regional and global literature comparison

To compare changes in nannofossil assemblages at El Kef to those at other Northern Hemisphere sites, we compiled a dataset using results published in the literature, which sample several different ocean basins and marine environments (Figure 1). The corresponding data used in these comparisons are from Bidart, France (Jiang et al., 2019); Zumaia, Spain (Jiang et al., 2019); Agost, Spain (Pospichal, 1995), Forada, Italy (Fornaciari et al., 2007), Wadi Hamama and Gebel Qreiya, Egypt (Tantawy, 2003) in the paleo-Tethys; the Chicxulub impact crater (IODP-ICDP Site M0077A), Mexico (Jones et al., 2019) and Brazos River, USA (Schueth, MS thesis, 2009) in the Gulf of Mexico; Shatsky Rise (ODP Site 1209) in the North Pacific Ocean (Alvarez et al., 2019) and IODP Sites U1403 and U1407 in the North Atlantic Ocean (Bown et al., 2023).

Statistical analyses

All of the statistical analyses outlined below were conducted on genus-level data, allowing for more reliable comparison of the nannofossil assemblage records compiled by different nannofossil workers whilst still showing meaningful paleoecological trends. Before statistical analyses were performed, the Hellinger transformation method was applied to the genus-level assemblage data.

All of the genus-level assemblage data by the column maximum, where the abundance of each taxon in a sample is divided by its maximum occurrence across all samples. This maximizes the importance of rare taxa which is vital in teasing apart differences and similarities between assemblages that are almost completely dominated by one abundant taxon (such as within the short-lived acmes).

To statistically analyze the temporal changes in nannofossil assemblages, we performed Nonmetric Multidimensional Scaling (NMDS) using the metaMDS function (vegan package should cite) in R. This iterative ordination technique uses a distance measure (in this case the Bray-Curtis dissimilarity) to assess the similarity between both samples and species in a dataset. The number of axes (dimensions) used is specific to each data matrix and is manually chosen by the user when the 'stress' value is reduced to a point where it plateaus (in this case 3 dimensions). The resulting ordination plots samples and species as scores on NMDS axes 1 and 2, which explain the greatest amount of variation between samples. we performed two separate NMDS analyses; one only using nannoplankton assemblages from Hole E and the other using assemblage data from both Holes E and C. We then performed a further NMDS analysis to determine whether there were any regional, global, or environmental (i.e. shelf vs. pelagic) trends in assemblages.

To test whether the changes in nannofossil assemblages and environmental variables were correlated, we performed a linear regression of the available geochemical data (bulk carbonate $\delta^{13}C$ and $\delta^{18}O$, bulk organic $\delta^{13}C$, % TOC, and % $CaCO_3$) on the NMDS sample scores using the envfit function in the vegan package (cite) in R. Because geochemical measurements were not always conducted on the same samples as the nannofossil assemblage counts, we interpolated the geochemical values for each of our nannofossil samples.

To determine the extent to which regional palaeoceanographic conditions played a role in the recovery of calcareous nannoplankton, we performed a two-way cluster analysis using the nannofossil assemblage data from El Kef and six other Tethyan sites. we performed a two-way cluster

analysis using the heatmap.2 function (gplots package should give a citation here for the package) in R (should really cite R core team here). A two-way cluster analysis was then performed using the Bray-Curtis distance measure and the complete linkage method for hierarchical clustering. This creates a dendrogram of species on the x axis and a dendrogram of samples on the y axis, with species clustering based on co-occurrence among samples and samples clustering due to similarities in nannofossil assemblage composition.

Results

Summary of trends at El Kef

As at most other Northern Hemisphere sites, nannofossil assemblages immediately following the K/Pg mass extinction (61 to 61.5 m) were dominated by the calcareous benthic resting cysts of dinoflagellates (*Cervisiella* spp.), the potential short-term survivor *Watznaueria barnesiae* (Bown, 2005), and minor reworked Cretaceous nannofossils. Observed above this are the characteristic series of high abundance, low diversity acmes (Fig. 2), which at El Kef we define as the *Neobiscutum* acme (~52.5 to 61 m), the *Futyania* acme (~35 to 52.5 m), and the *Praeprinsius* acme (~14.5 to 35 m).

Ecological turnover across the unconformity

A marked ecological turnover occurs at across the unconformity (Fig. 2a), when assemblages dominated by the first of the acme taxa (*Neobiscutum* spp.) are almost completely replaced by assemblages containing dominant *Futyania petalosa*, and increased abundances of the long-ranging Paleocene taxa *Cruiciplacolithus primus* and *Coccolithus pelagicus*. This ecological turnover coincides with a 2 ‰ positive excursion in the $\delta^{13}C$ values of bulk carbonate (Fig. 2b), a transient ~1 ‰ drop in bulk organic $\delta^{13}C$ values followed by a steady 2 ‰ increase to higher than pre-excursion values (Fig. 2d), a slight decrease in % TOC (Fig. 2e), and a large increase in % $CaCO_3$ (Fig. 2f). This dramatic shift in assemblage composition is also evident on the NMDS plots, with samples above and below the unconformity plotting on different sides of ordination space (Fig. 3). Linear regression of the external geochemical variables on the NMDS sample scores suggests that the transition between the *Neobiscutum* and *Futyania* acmes was strongly and significantly related to increased bulk carbonate $\delta^{13}C$ values (r^2=0.65, p=0.001) and % $CaCO_3$ (r^2=0.5, p=0.001), and negatively correlated to % TOC (r^2=0.59, p=0.001). The positive correlation between higher relative abundances of *F. petalosa* and an increase in the $CaCO_3$ content likely reflects the increased cell size and calcite volume of *F. petalosa* compared to *Neobiscutum* spp. (Alvarez et al., 2019).

Because the ecological turnover across the unconformity represents such a large shift in the dominant nannoplankton taxa, smaller changes that occurred before and/or after it might be obscured. For this reason, we chose to perform further, separate analyses on samples from below and above this stratigraphic horizon (Fig. 3).

Below the unconformity

With the exception of a short interval immediately following the K/Pg boundary (61-61.5 m), most of the sediments below the unconformity belong to the *Neobiscutum* acme. *Cervisiella* spp. (calcareous dinoflagellate cysts) are more abundant near the base of the acme (56.5 to 61 m) in the same depth interval where most of the geochemical records fluctuate, suggesting the environment was unstable or volatile. Between ~57 and 59 m, a peak in the abundance of *Braarudosphaera* spp., a taxon which is restricted to coastal regions in the modern ocean, coincides with a broad increase in both bulk carbonate and bulk organic $\delta^{13}C$ values. Decreased abundances of both *Cervisiella* spp. and *Braarudosphaera* spp. between 52.5 and 55 m are recorded in the same depth interval as: (a) increased abundances of tiny, ancestral *Praeprinsius* spp. (*Praeprinsius vegrandis*?), (b) decreased %

TOC and % CaCO3, (c) increased bulk organic $\delta^{13}C$ values, and (d) relative stasis in bulk carbonate $\delta^{13}C$ values.

Our NMDS results (Fig. 3) show that below 52.5 m, where *F. petalosa* is present but not yet abundant, most of the variation between nannoplankton assemblages can be explained by the presence or absence of the Cretaceous survivors *W. barnesiae* and *Zeugrhabdotus sigmoides*. However, these taxa are only present in a few of the basal samples. Above this, the relative abundance of *Neobiscutum* spp. vs. *F. petalosa* (and to a lesser extent, the relative abundance of *Braarudosphaera* spp.), drives the differences between samples. Samples with increased *F. petalosa* have a weak (but significant) stratigraphic time dependence (i.e. younger samples tend to have higher relative abundances of *F. petalosa*; r^2=0.35, p=0.001), higher bulk carbonate $\delta^{13}C$ values (r2=0.23, p=0.001) and higher % $CaCO_3$ (r^2=0.24, p=0.001).

Above the unconformity

For the first meter above the unconformity, nannoplankton assemblages are dominated by *F. petalosa*, with increased relative abundances of *C. primus* (Fig. 2). *F. petalosa* then gradually decreases in abundance until ~35 m. The progressive decline in *F. petalosa* is synchronous with a gradual increase in the abundance of *Praeprinsius tenuiculus*, which then becomes the dominant nannoplankton taxon from ~35 m to the top of the analyzed section.

Regressing environmental data on the NMDS scores for the entire dataset (Fig. 3b) results in a positive correlation between the *Futyania*/*Praeprinsius* acmes and % $CaCO_3$ (r^2=0.52, p=0.001), and a negative correlation with % TOC (r2=0.69, p=0.001) and bulk organic $\delta^{13}C$ values (r^2=0.56, p=0.001). However, isolating the post-52.5 m samples causes these relationships to completely collapse (Fig. 3d), indicating that the strong correlations in Fig. 3b are driven by the major nannoplankton turnover at 52.5 m. Unfortunately, there is not yet a bulk carbonate $\delta^{13}C$ or $\delta^{18}O$ record for the interval above 52.5 m. However, by using the currently available geochemical data, it appears that the transition from the *Futyania* acme to the *Praeprinsius* acme may not have been as dependent on environmental (i.e. abiotic) factors.

Regional trends

To assess similarities between K/Pg nannofossil assemblages at El Kef and four other Tethyan sites (Gebel Qreiya and Wadi Hamama, Egypt; Agost, Spain; and Forada, Italy), we performed a two-way cluster analysis. Results indicate that samples form two main clusters (A and B; Fig.4) based on their stratigraphic age/height. To help further interpret our results, we also used the estimated paleo-water depths for each site from Jiang et al. (2010), which were modified after Keller, 1996.

Major cluster B (the earlier recovery) can be subdivided into four secondary clusters (clusters 4 to 7). The first of these (cluster 4) contains samples from all of the included Tethyan sites and represents the immediate post-impact assemblages which are observed worldwide. These assemblages are primarily dominated by fragments belonging to the calcareous cysts of dinoflagellates (*Cervisiella* spp.), with some samples from Gebel Qreiya and Agost separating out further due to higher abundances of other Cretaceous survivors such as *W. barnesiae* and *Markalius inversus*.

Cluster 5 contains samples within the *Braarudosphaera* acme, which is present to some degree at all of the Tethyan sites apart from El Kef. This is unusual because *Braarudosphaera* spp. is generally considered to be a eutrophic-adapted taxon, so would be expected to have higher abundances closer to the continental shelf. However, in this analysis, *Braarudosphaera* spp. has its lowest abundance at El Kef, which samples an outer shelf/upper-slope environment (200-300 m paleowater depth) that is

similar to Agost, and is shallower than Forada which was likely characterized by pelagic conditions (>1500 m paleo-water depth). Instead, samples from El Kef (and a few from Agost) separate out due to the almost complete dominance of *Neobiscutum* spp. during the earlier recovery (cluster 7). This taxon only appears to form acmes at the outer shelf/upper slope sites (200-500 m paleo-water depth), suggesting that it was restricted to these environments in the paleo-Tethys.

The last sub-cluster (6) in major cluster B, consists solely of samples from Forada which is the only site included in this analysis with a *Coccolithus* pelagicus acme. As *C. pelagicus* is known to be an oligotrophic taxon in the modern ocean, its dominance at Forada is consistent with the interpretation that this site represents a pelagic environment with relatively low surface ocean nutrient concentrations.

Care must be taken when attempting to interpret major cluster A (the later recovery), because *Futyania petalosa* coccoliths often resemble fragments of calcareous dinoflagellate cysts, meaning their abundance may have been underestimated in the literature, especially in earlier studies (e.g., Pospichal, 1994) when its identification was yet to be well-established. In addition, most authors did not analyze assemblages to the stratigraphic age/height we managed in this study. Nonetheless, there are still some patterns that can be recognized.

Firstly, *Cruciplacolithus primus* (sub-cluster 1), a long-ranging oligotrophic taxon, was more abundant at almost all of the other Tethyan sites compared to El Kef. Minor *C. primus* acmes were even present at Gebel Qreiya and Wadi Hamama (<200 m paleo-water depth), but were absent at El Kef (200-300 m paleo-water depth), which was further from the continental shelf and thus predicted to be more oligotrophic. This suggests that regional differences in post-extinction nannoplankton assemblages were not just controlled by position along a neritic-pelagic transect.

In the last two sub-clusters (2 and 3), samples separate out based on whether they fall within the *Praeprinsius* (cluster 2) or *Futyania* (cluster 3) acme. Due to the lack of stratigraphic resolution at most of the other Tethyan sites included in this study, it is difficult to ascertain whether *F. petalosa* was actually unusually dominant at El Kef and/or restricted to this site. However, because the *Praeprinsius* acme occurred after the *Futyania* acme at all other Northern Hemisphere sites, its absence at Forada (which contains samples from the *Praeprinsius* acme) likely reflects a true signal. This indicates that *F. petalosa* may not have been well-adapted to pelagic environments, which coupled with its dominance at El Kef, supports a previous interpretation (Jones et al., 2019) that *F. petalosa* was adapted to moderate nutrient levels (i.e. was a 'mesotrophic' taxon).

Global trends

Dissimilarity in K-Pg nannoplankton assemblages can also be examined on a global scale using NMDS (Figs. 5 and 6). Based on the major differences observed in the regional cluster analysis (Fig. 4), the sample scores for El Kef were separated from those for the other Tethyan sites.

Fig. 5 shows that the post-impact assemblage composition and 'recovery trajectories' at most Tethyan sites were very similar to those at "ground zero" of the Chicxulub crater (Ref. needed here). In contrast, the ecological sequences at El Kef were unique. Immediately following the 'disaster' assemblage dominated by inorganic dinoflagellate cysts, nannoplankton assemblages at El Kef were characterized by a nearly monospecific *Neobiscutum* acme (Fig. 6b). Besides a few occurrences at Shatsky Rise (North Pacific) and Agost (Tethys), the only other site to approach the almost complete dominance of *Neobiscutum* spp. at El Kef was Brazos River, Texas (Fig. 6b), a continental shelf site in the Gulf of Mexico (Fig. 5a). Because *Neobiscutum* spp. appears to have generally been restricted to shelf to upper-slope settings (<200-500 m paleo-water depth) with only sporadic occurrences in pelagic environments (Fig. 5b), it seems likely that this was a eutrophic-adapted taxon.

The *Neobiscutum* acme was directly followed by the *Futyania* acme at El Kef. *F. petalosa* was unusually abundant at this site (Fig. 6c), suggesting that it was very well-adapted to the environmental and/or ecological conditions which existed in that locale at the time. Other sites with lower (but significant) abundances of *F. petalosa* include Walvis Ridge (South Atlantic), Chicxulub, and Brazos River, Texas (Gulf of Mexico). The fact that *F. petalosa* was rare (or absent) at pelagic sites and shelf sites (>1000 m and <200 m paleo-water depths, respectively), supports that it was a mesotrophic taxon.

By the top of the studied section at El Kef, nannoplankton assemblages fall within the *Praeprinsius* acme. This marked the end of post-impact regional heterogeneity in nannoplankton assemblages (citation?), as *Praeprinsius* tenuiculus was consistently abundant at all of the included sites (Fig. 6d). Therefore, despite consisting of a distinct series of nannoplankton taxa, the boom-bust successions at El Kef support previous interpretations that taxonomic switchovers were driven by a decrease in surface ocean nutrients.

Taxa that were not as abundant at El Kef compared to elsewhere are *Braarudosphaera* spp. (Fig. 6a), *Cruciplacolithus primus* (Fig. 6e), and *Coccolithus pelagicus* (Fig. 6f). *Braarudosphaera* spp. has a very spotty occurrence, and was predominantly restricted to the Tethyan Ocean and the Gulf of Mexico (Fig. 5a). Despite commonly being referred to as a neritic taxon, the sites where *Braarudosphaera* spp. were abundant span a range of paleo-water depths (<200 to >1500 m), which is inconsistent with this interpretation. This either indicates that hemipelagic/pelagic environments in the paleo-Tethys and Gulf of Mexico were unusually eutrophic during the early recovery, or that a different ecological or environmental variable was driving the abundance of *Braarudosphaera* spp. in these regions.

The other two taxa that do not form acmes at El Kef are *C. primus* and *C. pelagicus*, which were likely oligotrophic-adapted based on the biogeographic distribution of modern *C. pelagicus*, and were thus predominant in pelagic environments (Fig. 5b). As expected, this caused an overwhelming dominance of *C. primus* at Shatsky Rise (Fig. 6e), and relatively high abundances of *C. pelagicus* at Shatsky Rise, Walvis Ridge, and Forada (pelagic Tethyan site; Fig. 6f).

Discussion

Ecological change at El Kef

Our dataset provides the opportunity to explore the mechanisms that drove ecological reorganization at the base of the marine food web, following the biggest mass extinction event in the last 250 million years of Earth history. In addition, the high sedimentation rates at El Kef allow us to examine ecological change at a higher resolution (every ~5000 years based on the available planktic foraminifera biozone datums) than can be achieved at commonly studied pelagic sites which are generally stratigraphically condensed. Below, we explore the four stages of ecological turnover within nannoplankton communities following the K-Pg impact at El Kef and discuss the potential mechanisms that drove these taxonomic switchovers.

Stage 1: The cyst acme (61 to 61.5 m composite core depth)

We find a significant ecological reorganization in the plankton, from latest Maastrichtian communities dominated by calcareous nannoplankton to earliest Danian assemblages characterized by non-calcifying opportunists that were able to form resting cysts. As in previous studies, our results show that nannoplankton assemblages immediately following the impact were dominated by the calcareous resting cysts of dinoflagellates such as *Cervisiella* spp., which did not suffer a mass extinction at the K-Pg boundary (e.g., Brinkhuis and Zachariasse, 1988; Habib et al., 1992; Slimani et al., 2010). Because dinoflagellates usually produce calcareous or organic-walled cysts in response to suboptimal growth conditions (e.g., Bravo and Figueroa, 2014) such as fluctuating temperatures or

rapidly changing nutrients (Fig. 2c; Brinkhuis et al., 1998; Vellekoop et al., 2015), their increase in abundance indicates that the surface ocean at El Kef was an unstable and often inhospitable habitat during the first ~40,000 years of the Danian. Other phytoplankton groups such as diatoms, non-calcifying haptophytes, and cyanobacteria were also able to encyst and lay dormant on the seafloor, perhaps for as long as 100 years (e.g., Livingstone and Jaworski, 1980; McQuoid et al., 2002; Hämström et al., 2011; Ribeiro et al., 2011). These organisms were provided with an opportunity to infiltrate vacated niche space and take advantage of unused resources shortly after the K-Pg impact (Hollander et al., 1993; Brinkhuis et al., 1998; Hildebrand-Habel and Streng, 2003) due to the extinction of 93% of calcareous nannoplankton, which were arguably the most dominant primary producers during the Mesozoic (Knoll and Follows, 2016). Therefore, it is unlikely that there was a complete loss of primary productivity at the K-Pg boundary (e.g., D'Hondt et al., 1998; Sepúlveda et al, 2009; Alegret et al., 2012, Sepúlveda et al., 2019). The significant reorganization of primary producers likely had far-reaching impacts on the structure of marine food webs, and the strength and efficiency of export productivity.

Stage 2: The Neobiscutum acme (52.5 to 61 m composite core depth)

Following the relatively brief (<40,000 years) interval of environmental stress at El Kef, the first of the nannoplankton boom-bust taxa (*Neobiscutum* spp.) floods samples and becomes dominant (Fig. 2a). The near-complete elimination of nannoplankton at the K-Pg boundary followed by a brief interval of slight ecosystem recovery during Stage 1 may have allowed the opportunistic taxon *Neobiscutum* spp. to proliferate into newly vacant niche space. The opening of niche space may explain the increased dominance of previously rare Cretaceous survivors such as *Cyclagelosphaera reinhardtii*, *Zeugrhabdotus sigmoides*, and *Markalius inversus* in early Paleocene nannoplankton assemblages from Southern Hemisphere sites (Schueth et al., 2015). These Cretaceous survivors are only a very minor component of nannoplankton assemblages at El Kef, likely due to overall higher extinction rates in the Northern vs. Southern Hemisphere (Jiang et al., 2010). Although *Neobiscutum* spp. is commonly considered a newly evolved Paleocene taxon, the rate at which it proliferated and thrived following the K-Pg boundary supports earlier work suggesting this taxon was also a Cretaceous survivor which was present but very rare in Northern Hemisphere assemblages during the latest Maastrichtian (Mai et al., 2003).

What gave the tiny, weakly calcified genus *Neobiscutum* a competitive advantage over other surviving coccolithophore genera is uncertain. One possibility is that a decrease in biological pump efficiency immediately following the K-Pg impact (e.g., D'Hondt et al., 1998; Coxall et al., 2006; Birch et al., 2016), drove increased remineralization in the upper water column, leading to higher nutrient availability. Most of the nannoplankton taxa that became extinct were cosmopolitan species adapted to low-nutrient (oligotrophic) environments (e.g. Jiang et al., 2010). In contrast, *Neobiscutum* may have been a eutrophic-adapted genus that selectively survived the mass extinction event and was able to thrive in the high-nutrient surface waters that existed thereafter. The resulting high abundance, low diversity assemblages that formed in response to elevated nutrient availability (Fig. 2a) are reminiscent of modern, eutrophic environments (Okada and Honjo, 1973), which supports this interpretation.

In addition to favouring eutrophic conditions, it is possible that the tiny cell size and low biomineralization potential of *Neobiscutum* spp. (Alvarez et al., 2019) provided it with a further competitive advantage. At the base of the *Neobiscutum* acme (from ~58 to 61 m composite core depth), δ^{13}Corg values remain consistently high (~-26.5 ‰). Because terrestrially-derived organic material was only a significant component of sediments for the first few centimeters above the K-Pg

boundary (reference needed here), we suggest that these high $\delta^{13}C$ values indicate that primary productivity continued to be provided by alternative (non-coccolithophore) phytoplankton groups, which were likely outcompeting nannoplankton and using most of the available macronutrients. Evidence for increased dinoflagellate primary productivity in Tunisian shelf settings (El Kef and the nearby Elles section) includes increased absolute abundances of dinocysts in the early Danian, as well as a relative increase in the percentage of peridinioid dinoflagellates that tend to thrive in high productivity environments (e.g., Brinkhuis et al., 1998; Sluijs et al., 2005; Vellekoop et al., 2015). Coccolithophores are at a competitive disadvantage in unstable (i.e. disturbed) and/or high-nutrient environments today (e.g., Tozzi et al., 2003; Litchman, 2007; Endo et al., 2018). Having a smaller cell size and thus a larger surface area to volume ratio, as *Neobiscutum* spp. did, could be advantageous in the diffusion of CO_2 into the cell during photosynthesis, especially in highly productive environments that have a high CO_2 demand (e.g., Taucher et al., 2015; Basu and Mackey, 2018). The unusually small cell size and tiny, thin calcite plates of *Neobiscutum* spp. also suggest that it was able to divide (i.e. reproduce) very quickly (e.g., Gibbs et al., 2013; O'Dea et al., 2014; Sheward et al., 2017; Gibbs et al., 2018), allowing it to more rapidly proliferate and bloom compared to typical coccolithophore species under unfavorable environmental conditions, a phenomenon potentially analogous to *Emiliania huxleyi* blooms in the modern ocean (Paasche, 2001; Buitenhuis et al., 2008; Langer et al., 2009; Daniels et al., 2014).

Although *Neobiscutum* is almost completely dominant for the entirety of its acme, there is a small (< 20%) spike in the relative abundance of the neritic, eutrophic taxon *Braarudosphaera* spp. (Perch-Nielsen, 1985; Kelly et al., 2003; Liebrand et al., 2018) between ~57 and 59 m composite core depth (Fig. 2a). Significantly, this peak in abundance is synchronous with a transient ~2 ‰ increase in $\delta^{13}C_{carb}$ values, and a ~1 ‰ decrease in $\delta^{18}O_{carb}$ values (Fig. 2b, c). These trends can be interpreted in three different ways. Firstly, large fluctuations in both $\delta^{13}C_{carb}$ and $\delta^{18}O_{carb}$ values suggest environmental volatility that *Braarudosphaera* spp. may have been better adapted to than *Neobiscutum* spp. This would be supported by a relatively high abundance of *Cervisiella* cysts during this interval. Secondly, the fluctuation in isotopic records may simply represent the increased contribution of *Braarudosphaera* calcite to the bulk carbonate. *Braarudosphaera* spp. unlike most other coccolithophores, calcifies extracellularly (Hagino et al., 2016), meaning that it may fractionate oxygen and carbon isotopes differently to other haptophytes. Thirdly, the increased abundance of *Braarudosphaera* spp. and potential cyclic fluctuation in isotopic records, may be indicative of a temporary period of enhanced thermal stratification between 57 and 59 m. Short-lived *Braarudosphaera* acmes have been linked to orbitally-paced hyperstratification of the surface ocean (Liebrand et al., 2018). Also, the $\delta^{18}O_{carb}$ record at El Kef is consistent with transient warming during the time when *Braarudosphaera* spp. reached its maximum abundance (Fig. 2a). Above the interval of increased *Braarudosphaera* abundance, between 52.5 to 57 m, there was very little change in nannoplankton assemblages, with almost absolute dominance of *Neobiscutum* spp. This is coincident with relative stability in $\delta^{13}C_{carb}$ and $\delta^{18}O_{carb}$ records, both of which exhibit minor superimposed cyclical variability (Fig. 2b, c). This might lend support to the idea that the earlier increase in relative abundance of *Braarudosphaera* spp. between 57 and 59 m was due to lower tolerance of a period of environmental stress (i.e. volatile conditions) in *Neobiscutum* spp. relative to *Braarudosphaera* spp. at this time. This interval notwithstanding, the overwhelming dominance of *Neobiscutum* spp. throughout Stage 2 indicates that this taxon was remarkably well-adapted to conditions at El Kef during the early recovery.

Stage 3: Taxonomic switchover between the Neobiscutum and Futyania acmes (52.5 m composite core depth)

Stage 3 presents a significant turning point in the recovery of the marine ecosystem at El Kef. The abrupt taxonomic switchover between the *Neobiscutum* and *Futyania* acmes at 52.5 m is accompanied by: (a) a large (2.5 ‰) increase in $\delta^{13}C_{carb}$ values, (b) a sharp 1 ‰ decrease followed by a more gradual 2 ‰ increase in $\delta^{13}C_{org}$ values, (c) a 1 ‰ increase in $\delta^{18}O_{carb}$ values, and (d) a 3x increase in % $CaCO_3$ (Fig. 2b-d, f). The strong correlations between these ecological and geochemical data (Fig. 3) indicate that the nannoplankton boom-bust successions were intrinsically coupled to broader marine carbon cycling. Unfortunately, however, this turnover is also coincident with a sharp lithologic contact, which may represent a local condensed interval or erosional surface. For this reason, the apparently rapid decrease in the abundance of *Neobiscutum* at 52.5 m may not reliably reflect a true environmental or ecological signal. Despite these caveats, the taxonomic switchover between the *Neobiscutum* and *Futyania* acmes, regardless of whether it was driven by an ecological, environmental, or erosional mechanism is a true signal, as the same switchover is observed in two of the other El Kef cores (Supp. Fig.1), and the *Futyania* acme which is at the top of Hole E continues at the base of Hole C (Fig. 2).

There is some evidence that suggests the abruptness of the ecological turnover may in fact reflect a real environmental signal. Firstly, the sharp transition from dark, clay-rich marlstones dominated by *Neobiscutum* spp., to white, carbonate-rich sediments with abundant *Futyania petalosa* are a common feature in all three of the El Kef holes which capture this time interval (Supp. Fig. 2). This rules out the possibility that the taxonomic switchover is simply an artifact of drilling disturbance in Hole E, as otherwise these same patterns would not also have been observed in Holes A and D. Secondly, the abrupt increase in δ^{18}Ocarb values between ~52.55 and 52.75 m composite core depth actually occurs before the ecological turnover (between ~52.35 and 52.45 m), during an interval where there is no evidence for weathering or erosion. Thirdly, major weathering at the top of Hole E does not occur until a composite core depth of ~51.25 m. When samples from the weathered unit in Hole E were removed from our dataset (~49.3 to 51.25 m), the nannoplankton assemblages and geochemical records at the top of Hole E match up almost exactly with those at the base of Hole C. Thus, regardless of the rapidity or the mechanisms involved in driving the turnover, this taxonomic switchover resulted in a semi-permanent regime shift to a new steady state.

If a true signal, the direction of the trends in our geochemical data can be used to provide a plausible explanation for the apparent abruptness of the ecological turnover at ~52.5 m. Firstly, the large ~1 ‰ decrease in $\delta^{18}O_{carb}$ values before the turnover horizon, indicates an abrupt warming event, not previously observed in the fossil record, which could have driven enhanced ocean stratification. Increased ocean stratification would have created a more 'stable', lower nutrient surface water environment due to decreased vertical mixing and thus reduced nutrient replenishment from depth. Nutrients in the surface ocean were then efficiently utilized by the existing community of highly productive, opportunistic phytoplankton. As the waters became more stratified and nutrient availability decreased, the surface ocean at El Kef eventually would have crossed a threshold, whereby the early recovery phytoplankton community was displaced due to increased competition with coccolithophores, which likely had a competitive advantage in this new, relatively stable, oligotrophic environment (e.g., Tozzi et al., 2003; Litchman, 2007; Endo et al., 20[18]). Lower nutrient availability would have also caused an overall decrease in primary productivity. Decreased primary productivity is supported by: (a) an initial decrease in $\delta^{13}C_{org}$ values (Fig. 2d), which may have been caused by an increase in the isotopic fractionation of carbon during photosynthesis (e.g., Freeman and Hayes, 1992), and (b) the transition to a higher diversity nannoplankton assemblage (Fig. 2a), which is indicative of a more oligotrophic environment (Okada and Honjo, 1973).

Along with these changes, it is probable that there was a synchronous shift in the efficiency of the biological pump, which is best expressed by the isotopic gradient between the $\delta^{13}C$ values of planktic and benthic foraminifera. Although these data are not currently available at El Kef, the large, ~2.5 ‰ increase in $\delta^{13}C_{carb}$ values (and concurrent increase in $\delta^{13}C_{org}$ values), is consistent with increased biological pump efficiency (Birch et al., 2016). Reduced remineralization of organic matter in the upper water column would have increased the carbonate saturation state, making it easier for calcifying organics to precipitate calcite. This, coupled with lower primary productivity and thus a decreased demand for carbon dioxide, would have favored the proliferation of larger, more heavily calcified nannoplankton taxa such as *Futyania petalosa* and *Cruciplacolithus primus*, as reflected by the 3 x increase in % $CaCO_3$ at 52.5 m (Fig. 2f).

The cause of the sudden increase in biological pump efficiency is uncertain. One possibility is that the decrease in overall primary productivity driven by stratification, led to a lower absolute abundance of organic matter in the upper water column. Therefore, even if export productivity remained the same (e.g., a strong biological pump), a higher proportion of the upwelled organic carbon was still transported out of the surface ocean. A second possibility is that increased biological pump efficiency was a direct result of the recovery of organisms at higher trophic levels (e.g., copepods) which were able to form aggregates. This would have increased the sinking speed of organic matter, thereby decreasing surface water nutrient concentrations and causing the phytoplankton turnover (i.e. the 'Living Ocean' model of D'Hondt et al., 1998). Alternatively, it is possible that it was the phytoplankton turnover itself, caused by increased ocean stratification, which enhanced biological pump efficiency. A shift from dominant non-calcifying organisms to calcifying haptophytes (reflected in the decrease and sustained low values of $\delta^{13}C_{org}$ values above 52.5 m) may have improved the effectiveness of biomineral ballasting (Alvarez et al., 2019), which helped to remove a higher proportion of organic material from the surface ocean. Therefore, although we cannot discern whether the ecological reorganization within the phytoplankton was the cause or effect of increased biological pump efficiency, they would have likely interacted with each other in a positive feedback loop, thus leading to the establishment of a stable, lower-nutrient environment with a relatively diverse nannoplankton community.

Stage 4: The Futyania and Praeprinsius acmes (15 to 52.5 m composite core depth)

The relative quiescence of the ecosystem following the turnover horizon at 52.5 m is supported by the consistent nannoplankton assemblages up to a composite core depth of ~35 m. These nannoplankton assemblages were dominated by *Futyania petalosa*, with a steady but gradual increase in the relative abundance of *Praeprinsius* tenuiculus, and stable abundances of *C. primus* and *C. pelagicus*. This interval was accompanied by only very minor fluctuations in geochemical records, indicating a period of relative ecological and environmental stability.

The switchover between *F. petalosa* and *P. tenuiculus* occurs between ~30 and 35 m and is more gradual than the transition from the *Neobiscutum* to the *Futyania* acme (Fig. 2a). This ecological shift is not significantly correlated to any of the available geochemical records (Fig. 3), indicating that it was either caused by an environmental perturbation that is not recorded in our proxy data, or that this transition (in contrast to the last) was primarily driven by biotic rather than abiotic processes. Regardless of the cause, our nannoplankton data and geochemical records demonstrate that the switchover between the *Neobiscutum* and *Futyania* acmes resulted in a larger, more extreme regime shift compared to the switchover between the *Futyania* and *Praeprinsius* acmes (Figs. 2, 3).

Regional trends in nannoplankton assemblages

The regional cluster analysis (Fig. 4) and global NMDS results (Fig. 5) indicate that the series of taxa that formed boom-bust successions were both locally and regionally distinct. In the paleo-Tethys, samples from El Kef cluster separately from most other sites for the duration of the studied interval. In the earlier recovery, this is partially driven by the reduced dominance of 'disaster' taxa such as *Cervisiella* spp. at El Kef compared to the other Tethyan sites, suggesting that environmental instability was not as prevalent or prolonged at El Kef.

Surface ocean nutrient concentrations were regionally high in the paleo-Tethys throughout the early recovery, as indicated by the dominance of *Braarudosphaera* spp. at Agost (Spain), Forada (Italy), and Wadi Hamama and Gebel Qreiya (Egypt), and *Neobiscutum* spp. at El Kef. The sustained dominance of *Neobiscutum* spp. at El Kef over a ~8 m depth interval, coupled with relatively low abundances of *Braarudosphaera* spp., appears to be an atypical signal for paleo-Tethyan sites. The minor contribution of *Braarudosphaera* spp. to nannoplankton assemblages at El Kef was not completely driven by differences between neritic and pelagic environments, as sites with greater paleodepths (e.g., Agost and Forada) were also characterized by dominant *Braarudosphaera* spp. This indicates unique local environmental conditions at El Kef that may have been partially caused by differences in oceanographic processes between the northern and southern Tethyan margins (southern Eurasia and northern Africa, respectively), such as unstable, eutrophic conditions in the northern Tethys, to which *Braarudosphaera* spp. was well-adapted. Similar local environmental conditions may have existed at neritic sites in the southern Tethys (e.g., Wadi Hamama and Gebel Qreiya), with deeper locations (e.g., El Kef) characterized by more stable, slightly less eutrophic environments, which favored the proliferation of *Neobiscutum* spp. over *Braarudosphaera* spp.

A switchover between eutrophic and more oligotrophic taxa occurred at all sites during the later recovery, which supports the previous interpretation that taxonomic switchovers in boom-bust successions were driven by a decrease in surface ocean nutrients and a more efficient biological pump (Jones et al., 2019). However as with the earlier recovery, the nannoplankton taxa that comprise the later boom-bust acmes were locally distinct. Most of the Tethyan sites, regardless of marine environmental or geographical location, were dominated by *C. primus* and/or *C. pelagicus* during the later recovery. Although *C. primus* and *C. pelagicus* were both present at El Kef, *Futyania petalosa* was the dominant nannoplankton species at this site. It is possible that the relatively low abundances of this taxon at other Tethyan sites is simply a result of misidentification (especially in the older studies), as *F. petalosa* coccospheres resemble *Cervisiella* cysts, and individual *F. petalosa* coccoliths are visually similar to cyst fragments. However, if *F. petalosa* was unusually abundant at El Kef compared to other Tethyan sites (Fig. 5), this suggests that it was particularly well adapted to the environmental and/or ecological conditions that prevailed here during this time. The fact that *F. petalosa* was possibly rare (or absent) at pelagic and shelf sites (<200 m and >1000 m paleo-water depths) also supports previous interpretations that it was adapted to the moderate nutrient concentrations which were likely prevalent in outer shelf/upper slope environments (Jones et al., 2019).

Regionally distinct nannoplankton assemblages during the post-extinction interval were potentially driven by the westward-flowing Tethyan Circumglobal Current (TCC; Puceat et al., 2005; Soudry et al., 2006), which would have caused paleogeographic differences throughout the Tethyan basin. The strength of the TCC in the south-eastern Tethys would have produced intense upwelling, leading to eutrophic, high productivity ecosystems in these regions including the Egyptian shelf and slope (Soudry et al., 2006). As the TCC moved westward, nutrients would have been diminished, meaning that in areas in present day North Africa (including El Kef) upwelling may have been less nutrient-rich (Soudry et al., 2006). Although this is incompatible with benthic foraminiferal indicators of upwelling and high nutrient concentrations at nearby Elles, Tunisia (Coccioni and Marsilli, 2007), El Kef was

located further from the continental shelf than Elles (Karoui-Yaakoub et al., 2002; Adatte et al., 2002), and therefore likely experienced less upwelling. Modelling studies (e.g., Bush, 1997) and geochemical evidence from neodymium isotopes (Puceat et al., 2005) suggest that a weaker, eastward flowing current may have also been established during monsoon season, driving seasonal upwelling along the southern coast of Eurasia.

To summarize, there are significant local differences in calcareous nannoplankton assemblages within the paleo-Tethys, especially when considering the relative abundances of Cretaceous survivors (particularly *Braarudosphaera* spp.), and the boom-bust taxa *Neobiscutum* spp., *F. petalosa*, *C. primus*, *C. pelagicus*, and *P. tenuiculus*. These differences are likely a product of the relative position of sites along the shelf-slope transect, which in combination with ocean circulation led to variations in upwelling intensity. Sites that experienced more upwelling, including shelf sites and sites located in the south-eastern Tethys, would have been more environmentally volatile and had higher surface ocean nutrient concentrations than slope sites, driving the increased dominance of *Braarudosphaera* spp. at these locales.

Global trends in nannoplankton assemblages

The global NMDS results (Fig.5; Fig. 6) support our interpretations that *Futyania petalosa* was uniquely adapted to shelf slope environments, and that the dominance of *Braarudosphaera* spp. was not simply a neritic signal, but a product of local or regional paleoceanographic and/or paleoenvironmental processes that led to high levels of environmental stress at certain sites (e.g., most of the paleo-Tethyan Ocean and Chicxulub). Nevertheless, there is a clear shelf vs. open-ocean signal in our data. For example, *Neobiscutum* spp. was dominant in relatively stable shelf-slope environments (e.g., El Kef and Brazos River) but only formed short-lived blooms at pelagic sites such as Shatsky Rise. Instead, Shatsky Rise was dominated by *Cruciplacolithus primus*, which was only a minor component of assemblages at all other sites. This taxon is generally considered to be oligotrophic, and likely dominated in environments with a lower nutrient availability (i.e. pelagic sites). However, Walvis Ridge, which is also a pelagic site, saw only low abundances of *C. primus*. This is likely due to the incumbency of previously rare Cretaceous survivors at Walvis Ridge (Schueth et al., 2015), which highlights that ecological and environmental processes were equally important in driving the globally heterogeneous recovery of nannoplankton assemblages following the K-Pg mass extinction event. Therefore, although global differences between nannoplankton boom-bust successions were primarily driven by the type of marine environment represented (e.g., shelf vs. slope vs. open-ocean), superimposed local/regional ecological and oceanographic processes added extra complexity to the observed recovery patterns.

The significance of boom-bust successions

The occurrence of high abundance, low diversity acmes after the K-Pg boundary is observed in other fossil groups. Compared to nannoplankton, planktic foraminifera diversified rapidly (e.g., Hull et al., 2011; Lowery et al., 2018), but their post-extinction evolutionary trajectory from eutrophic scavengers (microperforate forms) to symbiont-bearing taxa is also consistent with ecological reorganization, which was intrinsically linked to a gradual decrease in surface ocean nutrient availability and more efficient biological pumping (e.g., Coxall et al., 2006; Jones et al., 2019; Lowery et al., 2021). Similar trends are also observed in the Benthic foraminifera did not suffer mass extinction at the K/Pg boundary, but diversity of their assemblages decreased globally (e.g., Alegret and Thomas, 2005; Thomas, 2007; Alegret et al., 2012). Blooms of both infaunal and epifaunal benthic foraminifera species have also been identified immediately above the K/Pg boundary at sites globally distributed, including at El Kef (Speijer and Van der Zwaan, 1996; Alegret, 2008) and other

Tethyan sections (e.g., Coccioni et al., 1993; Alegret et al., 2003), which have been interpreted as the response to the arrival of food from short-lived, local blooms of primary producers.

Changes in trophic strategy are also observed in molluscs, most noticeably by the transition from bivalve to gastropod-dominated assemblages across the K-Pg boundary (e.g., Valentine, 1969; Vermeij, 1977; Sepkoski, 2002; Alroy, 2010). Bivalves also experienced significant shifts in their dominant modes of life, due to the preferential survival (and origination) of taxa which were motile, and had an infaunal, deposit/filter feeding life habit (e.g., Aberhan et al., 2007; Sessa et al., 2012; Whittle et al., 2019). At some sites, especially in the Southern Hemisphere, previously rare Cretaceous bivalves which survived the mass extinction became locally incumbent (Hansen, 1988; Aberhan and Kiessling, 2014), which mirrors the ecological patterns in nannoplankton recovery (Schueth et al., 2015). At other sites, one to three species of particularly well-adapted bivalve taxa 'bloomed' to form high abundance, low diversity assemblages (Hansen, 1988; Aberhan et al., 2007; Aberhan and Kiessling, 2014; Witts et al., 2016; Whittle et al., 2019). These assemblages (which persisted for 200-300 kyr) were followed by a period of diversification, and an eventual transition to stable assemblages dominated by suspension feeders ~2 to 3 Myr post-impact (Hansen et al., 1993; Sessa et al., 2012; Whittle et al., 2019). As with the nannoplankton boom-bust successions, patterns in the ecological reorganization of bivalves were temporally and spatially heterogeneous, with inter-site variability unrelated to distance from the Chicxulub impact crater, latitude, or ocean basin (Aberhan et al., 2007; Sessa et al., 2012; Aberhan and Kiessling, 2014; Aberhan and Kiessling, 2015; Witts et al., 2016; Whittle et al., 2019).

Previous work has suggested that despite these heterogeneities, the direction of the trend in bivalve recovery patterns is globally homogeneous, thus indicating that a deterministic (as opposed to a stochastic) mechanism was responsible for ecological reorganization (Aberhan and Kiessling, 2015). The traditional explanation for this is a 'crash' in primary productivity, with inter-site variability caused by the differential effect of the impact on local environmental conditions (e.g., Rhodes and Thayer, 1991; Hansen et al., 1993; Sheehan et al., 1996; Aberhan et al., 2007). However, decreased primary productivity at the K-Pg boundary is not supported by the recent literature (e.g., Sepúlveda et al., 2009; Alegret et al., 2012; Lowery et al., 2018; Sepúlveda et al., 2019), with some sites experiencing a rapid recovery, or even an increase, in primary productivity after the impact.

That primary productivity remained high is also evidenced by the limited extinction of pelagic fish at the K-Pg boundary (Sibert et al., 2015; Sibert et al., 2018). However, there was also massive ecological reorganization within fish communities, including the increased dominance of ray-finned fish compared to sharks, perhaps related to the colonization of vacant niche space following the complete extinction of the ammonites (Sibert et al., 2015). In addition, the two fish teeth morphotypes that became extinct at the K-Pg boundary were two of the most dominant during the late Cretaceous (Sibert et al., 2018). Although small fish teeth were the dominant components of ichthyolith assemblages both during the late Maastrichtian and early Danian, there was a marked increase in tooth size at ~64 Ma, which is particularly prominent in the South Pacific (Sibert et al., 2015). Interestingly, this corresponds well with estimates of the time-scales over which the marine biological pump is thought to have recovered (e.g., D'Hondt et al., 1998; Coxall et al., 2006; Birch et al., 2016), although as with the other taxonomic groups discussed above, ecological reorganization within fish communities was globally heterogeneous (Sibert et al., 2015).

Patterns of ecological reorganization across different taxonomic groups and trophic levels (including in the calcareous nannoplankton, planktic foraminifera, benthic foraminifera, molluscs, and pelagic fish), indicate that a common cause drove post-impact 'recovery' patterns. Immediately following the mass extinction event, the biological pump collapsed. Although primary productivity remained high,

only a small percentage of the organic matter was transported to depth, leading to increased remineralization in the upper water column, thus higher nutrient availability and the prevalence of eutrophic-adapted plankton. This decreased efficiency in export productivity was likely caused by a combination of factors including the predominance of non-calcifying phytoplankton groups (Sepúlveda et al., 2009; Alegret et al., 2012), a reduction in the average size and biovolume of calcareous nannoplankton (Alvarez et al., 2019) and planktic foraminifera (e.g., Smit, 1982; Arenillas et al., 2018), and potentially, the increased dominance of ray-finned fish over sharks (Sibert et al., 2015), which may have led to less efficient packaging of fecal pellets to form large amalgamations of marine snow. The arrival of organic matter produced by non-calcifying phytoplankton groups to the seafloor, and the irregular food delivery through a succession of opportunistic blooms of primary producers, led to low-diversity assemblages of benthic foraminifera, characterized by quantitative peaks of opportunistic species that were able to cope with changes in the type of food (e.g., Alegret and Thomas, 2009, 2013).

The gradual recovery of biological pump efficiency, as evidenced by an increase in the vertical $\delta^{13}C$ gradient (e.g. Birch et al. 2016), coincides with: a) increased dominance of calcifying phytoplankton, switchovers in calcareous nannoplankton boom-bust successions to acmes containing larger, more heavily calcified taxa (Jones et al., 2019; Alvarez et al., 2019; this study), b) increased complexity of planktic foraminifer morphology and feeding strategies (Lowery and Fraass, 2019), and c) an increase in the diversity and maximum size of fish teeth (Sibert et al., 2015). This likely increased the efficiency of the biological pump through more efficient biomineral ballasting and the formation of larger fecal aggregates (if the size of fish teeth is directly correlated to body size; Sibert et al., 2015). The higher percentage of organic matter reaching the seafloor would have reduced the dominance of benthic infaunal taxa, allowing for the diversification of groups with alternative modes of life (especially suspension feeders). The exact causative mechanisms of the initial decrease in upper water column nutrient availability, and the timescales over which they occurred, would have depended greatly on local environmental conditions, leading to the observed global heterogeneity in ecological reorganization.

We propose that the decrease in surface ocean nutrient availability over millennia to millions of years after the mass extinction event triggered a regime shift that caused large-scale ecological turnover within the surface ocean across several different taxonomic groups. This played a major role in increasing biological pump efficiency, which in turn dictated the supply of nutrients to depth and the ecological reorganization of benthic communities. This apparent coupling between ecological recovery in the surface and deep ocean warrants further examination and speaks to the need for integrative “top-bottom” studies which focus on the co-dependence of planktic and benthic ecosystem recovery.

Conclusions

Our calcareous nannoplankton dataset provides the highest-resolution record yet from a K-Pg outer shelf-upper slope site, allowing us to gain a deeper perspective on the effect of mass extinction events on highly dynamic marine environments. We show that the boom-bust successions of newly evolved, short-lived nannoplankton taxa observed at other Northern Hemisphere K-Pg sites were also present at El Kef. Some of these boom-bust taxa (in particular *Neobiscutum* spp. and *Futyania petalosa*) seem to have been particularly well-adapted to the local environmental conditions at El Kef, being observed in higher abundances here than at all of the other K-Pg sites. We also identify a significant turnover in nannoplankton assemblages at ~52.5 m composite core depth, which coincides with a large, sustained increase in the $\delta^{13}C$ values of bulk carbonate. This suggests that the

nannoplankton turnover directly corresponded to increased biological pump efficiency, which in turn was caused by a transient warming event that enhanced vertical stratification.

Post-impact nannoplankton assemblages at El Kef were significantly different from those at other K-Pg sites in the paleo-Tethys, particularly with respect to the dominance of *Braarudosphaera* spp., a taxon which is commonly interpreted (REFS) as being adapted to stressed, neritic environments. Because paleo-water depths at El Kef are shallower than Tethyan sites with abundant *Braarudosphaera* spp., the low dominance of this taxon at El Kef indicates that it is more directly associated with eutrophic, rather than specifically upper-shelf environments. Lower nutrient availability at El Kef may have been related to the intensity of upwelling, which was likely weaker at El Kef compared to other shelf sites more proximal to land, and areas more directly affected by the Tethyan Circumglobal Current.

Our results support earlier findings that post-impact nannoplankton boom-bust successions were globally heterogeneous. Because distinct, regional-scale signals are not readily apparent, we suggest that this global disparity was primarily driven by differences in the pre-impact environment, as well as the unique paleoceanographic processes occurring in certain marine settings (i.e. pelagic vs. neritic environments). Ecological processes such as incumbency were also critical in shaping the structure of boom-bust successions on a local or regional scale (e.g., at Walvis Ridge), indicating that environmental conditions and ecology were equally important in the restructuring of nannoplankton communities following the K-Pg mass extinction event.

Remarkably, the patterns of ecological restructuring within the nannoplankton were very similar to those observed in other taxonomic groups such as the planktic foraminifera, benthic foraminifera, molluscs, and pelagic fish during the early Danian, suggesting they were all responding to the same environmental or ecological stimuli. This highlights the need for increased collaboration between researchers working on different taxonomic groups so as to more completely understand the ecosystem-scale responses to environmental change. As many of the after-effects of the K-Pg mass extinction are similar to processes occurring in the modern ocean, this type of studies will be particularly relevant in predicting how marine ecosystems may respond to anthropogenic activity.

829 **Literature cited**

830 Aberhan, M. and Kiessling, W., 2014. Rebuilding biodiversity of Patagonian marine molluscs after the
831 end-Cretaceous mass extinction. *PloS one*, e102629.
832 Aberhan, M. and Kiessling, W., 2015. Persistent ecological shifts in marine molluscan assemblages
833 across the end-Cretaceous mass extinction. *Proceedings of the National Academy of Sciences*,
834 *112*, pp.7207-7212.
835 Aberhan, M., Weidemeyer, S., Kiessling, W., Scasso, R.A. and Medina, F.A., 2007. Faunal evidence for
836 reduced productivity and uncoordinated recovery in Southern Hemisphere Cretaceous-
837 Paleogene boundary sections. *Geology*, *35*, pp.227-230.
838 Adatte, T., Keller, G. and Stinnesbeck, W., 2002. Late Cretaceous to early Paleocene climate and sea-
839 level fluctuations: the Tunisian record. *Palaeogeography, Palaeoclimatology, Palaeoecology*,
840 *178*, pp.165-196.
841 Alegret, L. and Thomas, E., 2005. Cretaceous/Paleogene boundary bathyal paleo-environments in the
842 central North Pacific (DSDP Site 465), the Northwestern Atlantic (ODP Site 1049), the Gulf of
843 Mexico and the Tethys: The benthic foraminiferal record. *Palaeogeography,*
844 *Palaeoclimatology, Palaeoecology*, *224*, pp. 53-82.
845 Alegret, L., Thomas, E. and Lohmann, K.C., 2012. End-Cretaceous marine mass extinction not caused
846 by productivity collapse. *Proceedings of the National Academy of Sciences*, *109*, pp. 728-732.
847 Alpert, P., Kishcha, P., Kaufman, Y.J. and Schwarzbard, R., 2005. Global dimming or local dimming?:
848 Effect of urbanization on sunlight availability. *Geophysical Research Letters*, *32*. Doi:
849 10.1029/2005gl023320.
850 Alroy, J., 2010. Geographical, environmental and intrinsic biotic controls on Phanerozoic marine
851 diversification. *Palaeontology*, *53*, pp. 1211-1235.
852 Alvarez, L.W., Alvarez, W., Asaro, F. and Michel, H.V., 1980. Extraterrestrial cause for the Cretaceous-
853 Tertiary extinction. *Science*, *208*, pp.1095-1108.
854 Alvarez, S.A., Gibbs, S.J., Bown, P.R., Kim, H., Sheward, R.M. and Ridgwell, A., 2019. Diversity
855 decoupled from ecosystem function and resilience during mass extinction recovery. *Nature*,
856 *574*, pp.242-245.
857 Arenillas, I., Arz, J.A. and Gilabert, V., 20^{18}. Blooms of aberrant planktic foraminifera across the K/Pg
858 boundary in the Western Tethys: causes and evolutionary implications. *Paleobiology*, *44*, pp
859 460-489.
860 Basu, S. and Mackey, K.R., 20^{18}. Phytoplankton as key mediators of the biological carbon pump: Their
861 responses to a changing climate. *Sustainability*, *10*, 869, doi: 10.3390/su10030869.
862 Berggren, W.A. and Pearson, P.N., 2005. A revised tropical to subtropical Paleogene planktonic
863 foraminiferal zonation. *The Journal of Foraminiferal Research*, *35*, pp.279-298.
864 Birch, H.S., Coxall, H.K., Pearson, P.N., Kroon, D. and Schmidt, D.N., 2016. Partial collapse of the
865 marine carbon pump after the Cretaceous-Paleogene boundary. *Geology*, *44*, pp.287-290.
866 Bown, P., 1998. *Calcareous nannofossil biostratigraphy* (pp. 1-315). Chapman and Hall; Kluwer
867 Academic.
868 Bown, P., 2005. Selective calcareous nannoplankton survivorship at the Cretaceous-Tertiary
869 boundary. *Geology*, *33*, pp.653-656.
870 Bown, P.R., Lees, J.A. and Young, J.R., 2004. Calcareous nannoplankton evolution and diversity
871 through time. In *Coccolithophores* (pp. 481-508). Springer, Berlin, Heidelberg.
872 Bravo, I. and Figueroa, R.I., 2014. Towards an ecological understanding of dinoflagellate cyst
873 functions. *Microorganisms*, *2*, pp. 11-32.
874 Brinkhuis, H., Bujak, J.P., Smit, J., Versteegh, G.J.M. and Visscher, H., 1998. Dinoflagellate-based sea
875 surface temperature reconstructions across the Cretaceous–Tertiary boundary.
876 *Palaeogeography, Palaeoclimatology, Palaeoecology*, *141*, pp.67-83.
877 Brinkhuis, H. and Zachariasse, W.J., 1988. Dinoflagellate cysts, sea level changes and planktonic
878 foraminifers across the Cretaceous-Tertiary boundary at El Haria, northwest Tunisia. *Marine*
879 *Micropaleontology*, *13*, pp.153-191.
880 Brown, W.L. and Wilson, E.O., 1956. Character displacement. *Systematic Zoology*, *5*, pp.49-64.

881 Brusatte, S.L., Lloyd, G.T., Wang, S.C. and Norell, M.A., 2014. Gradual assembly of avian body plan
882 culminated in rapid rates of evolution across the dinosaur-bird transition. *Current Biology*, *24*,
883 pp. 2386-2392.
884 Bush, A.B., 1997. Numerical simulation of the Cretaceous Tethys circumglobal current. *Science*, *275*,
885 pp. 807-810.
886 Coccioni, R. and Marsili, A., 2007. The response of benthic foraminifera to the K–Pg boundary biotic
887 crisis at Elles (northwestern Tunisia). *Palaeogeography, Palaeoclimatology, Palaeoecology*,
888 *255*, pp. 157-^{18}0.
889 Coxall, H.K., D'Hondt, S. and Zachos, J.C., 2006. Pelagic evolution and environmental recovery after
890 the Cretaceous-Paleogene mass extinction. *Geology*, *34*, pp.297-300.
891 D'Hondt, S., Donaghay, P., Zachos, J.C., Luttenberg, D. and Lindinger, M., 1998. Organic carbon fluxes
892 and ecological recovery from the Cretaceous-Tertiary mass extinction. *Science*, *282*, pp.276-
893 279. 119
894 Daniels, C.J., Sheward, R.M. and Poulton, A.J., 2014. Biogeochemical implications of comparative
895 growth rates of *Emiliania huxleyi* and *Coccolithus* species. *Biogeosciences*, *11*, pp. 6915-6925.
896 Endo, H., Ogata, H. and Suzuki, K., 20^{18}. Contrasting biogeography and diversity patterns between
897 diatoms and haptophytes in the central Pacific Ocean. *Scientific Reports, 8,* 10916.
898 Fornaciari, E., Giusberti, L., Luciani, V., Tateo, F., Agnini, C., Backman, J., Oddone, M. and Rio, D.,
899 2007. An expanded Cretaceous− Tertiary transition in a pelagic setting of the Southern Alps
900 (central-western Tethys). *Palaeogeography, Palaeoclimatology, Palaeoecology*, *255*, pp.98-
901 131.
902 Fraass, A.J., Kelly, D.C. and Peters, S.E., 2015. Macroevolutionary history of the planktic foraminifera.
903 *Annual Review of Earth and Planetary Sciences*, *43*, pp. 139-166.
904 Freeman, K.H. and Hayes, J.M., 1992. Fractionation of carbon isotopes by phytoplankton and
905 estimates of ancient CO2 levels. *Global Biogeochemical Cycles*, *6*, pp.^{18}5-198.
906 Gibbs, S.J., Poulton, A.J., Bown, P.R., Daniels, C.J., Hopkins, J., Young, J.R., Jones, H.L., Thiemann, G.J.,
907 O'Dea, S.A. and Newsam, C., 2013. Species-specific growth response of coccolithophores to
908 Palaeocene–Eocene environmental change. *Nature Geoscience*, *6*, pp.2^{18}-222.
909 Gibbs, S.J., Sheward, R.M., Bown, P.R., Poulton, A.J. and Alvarez, S.A., 20^{18}. Warm plankton soup and
910 red herrings: calcareous nannoplankton cellular communities and the Palaeocene–Eocene
911 Thermal Maximum. *Philosophical Transactions of the Royal Society A: Mathematical, Physical*
912 *and Engineering Sciences*, *376*, doi: 10.1098/rsta.2017.0075.
913 Habib, D., Moshkovitz, S. and Kramer, C., 1992. Dinoflagellate and calcareous nannofossil response to
914 sea-level change in Cretaceous-Tertiary boundary sections. *Geology*, *20*, pp.165-168.
915 Hagino, K., Tomioka, N., Young, J.R., Takano, Y., Onuma, R. and Horiguchi, T., 2016. Extracellular
916 calcification of *Braarudosphaera bigelowii* deduced from electron microscopic observations
917 of cell surface structure and elemental composition of pentaliths. *Marine Micropaleontology*,
918 *125*, pp. 85-94.
919 Hansen, T.A., 1988. Early Tertiary radiation of marine molluscs and the long-term effects of the
920 Cretaceous-Tertiary extinction. *Paleobiology*, *14*, pp. 37-51.
921 Hansen, T.A., Farrell, B.R. and Upshaw, B., 1993. The first 2 million years after the Cretaceous-
922 Tertiary boundary in east Texas: rate and paleoecology of the molluscan recovery.
923 *Paleobiology*, *19*, pp. 251-265.
924 Henehan, M.J., Ridgwell, A., Thomas, E., Zhang, S., Alegret, L., Schmidt, D.N., Rae, J.W., Witts, J.D.,
925 Landman, N.H., Greene, S.E. and Huber, B.T., 2019. Rapid ocean acidification and protracted
926 Earth system recovery followed the end-Cretaceous Chicxulub impact. *Proceedings of the*
927 *National Academy of Sciences*, *116*, pp.22500-22504.
928 Hildebrand-Habel, T. and Streng, M., 2003. Calcareous dinoflagellate associations and Maastrichtian–
929 Tertiary climatic change in a high-latitude core (ODP Hole 689B, Maud Rise, Weddell Sea).
930 *Palaeogeography, Palaeoclimatology, Palaeoecology*, *197*, pp. 293-321.

931 Hollander, D.J., McKenzie, J.A. and Hsü, K.J., 1993. Carbon isotope evidence for unusual plankton
932 blooms and fluctuations of surface water CO2 in “Strangelove Ocean” after terminal
933 Cretaceous event. *Palaeogeography, Palaeoclimatology, Palaeoecology*, *104*, pp. 229-237.
934 Hull, P.M., Bornemann, A., Penman, D.E., Henehan, M.J., Norris, R.D., Wilson, P.A., Blum, P., Alegret,
935 L., Batenburg, S.J., Bown, P.R. and Bralower, T.J., et al. 2020. On impact and volcanism across
936 the Cretaceous-Paleogene boundary. *Science*, *367*, pp.266-272.
937 Hull, P.M. and Norris, R.D., 2011. Diverse patterns of ocean export productivity change across the
938 Cretaceous-Paleogene boundary: New insights from biogenic barium. *Paleoceanography*, *26*,
939 PA3205.
940 Hull, P.M., Norris, R.D., Bralower, T.J. and Schueth, J.D., 2011. A role for chance in marine recovery
941 from the end-Cretaceous extinction. *Nature Geoscience*, *4*, pp.856-860.
942 Jiang, S., Bralower, T.J., Patzkowsky, M.E., Kump, L.R. and Schueth, J.D., 2010. Geographic controls on
943 nannoplankton extinction across the Cretaceous/Palaeogene boundary. *Nature Geoscience*,
944 *3*, pp.280-285.
945 Jones, H.L., Lowery, C.M. and Bralower, T.J., 2019. Delayed calcareous nannoplankton boom-bust
946 successions in the earliest Paleocene Chicxulub (Mexico) impact crater. *Geology*, *47*, pp.753-
947 756.
948 Keller, G., 1996. In*: Cretaceous-Tertiary mass extinctions: Biotic and Environmental changes,* eds.
949 MacLeod, N. & Keller, G., W. W. Norton & Company, New York, pp. 49-84.
950 Kelly, D.C., Norris, R.D. and Zachos, J.C., 2003. Deciphering the paleoceanographic significance of
951 Early Oligocene *Braarudosphaera* chalks in the South Atlantic. *Marine Micropaleontology*, *49*,
952 pp.49-63.
953 Knoll, A.H. and Follows, M.J., 2016. A bottom-up perspective on ecosystem change in Mesozoic
954 oceans. *Proceedings of the Royal Society B: Biological Sciences*, *283*, 20161755.
955 Langer, G., Nehrke, G., Probert, I., Ly, J. and Ziveri, P., 2009. Strain-specific responses of *Emiliania*
956 *huxleyi* to changing seawater carbonate chemistry. *Biogeosciences, 6*, 2637-2646.
957 Liebrand, D., Raffi, I., Fraguas, Á., Laxenaire, R., Bosmans, J.H., Hilgen, F.J., Wilson, P.A., Batenburg,
958 S.J., Beddow, H.M., Bohaty, S.M. and Bown, P.R., 20[18]. Orbitally Forced Hyperstratification of
959 the Oligocene South Atlantic Ocean. *Paleoceanography and Paleoclimatology*, *33*, pp.511-
960 529.
961 Litchman, E., Klausmeier, C.A., Schofield, O.M. and Falkowski, P.G., 2007. The role of functional traits
962 and trade-offs in structuring phytoplankton communities: scaling from cellular to ecosystem
963 level. *Ecology letters*, *10*, pp. 1170-1[18]1.
964 Livingstone, D. and Jaworski, G.H.M., 1980. The viability of akinetes of blue-green algae recovered
965 from the sediments of Rostherne Mere. *British Phycological Journal*, *15*, pp. 357-364.
966 Lowery, C.M., Bown, P.R., Fraass, A.J. and Hull, P.M., 2020. Ecological Response of Plankton to
967 Environmental Change: Thresholds for Extinction. *Annual Review of Earth and Planetary*
968 *Sciences*, *48*, doi: 10.1146/annurev-earth-081619-0528[18].
969 Lowery, C.M., Bralower, T.J., Owens, J.D., Rodríguez-Tovar, F.J., Jones, H., Smit, J., Whalen, M.T.,
970 Claeys, P., Farley, K., Gulick, S.P., Morgan, J.V., et al. 20[18]. Rapid recovery of life at ground
971 zero of the end-Cretaceous mass extinction. *Nature*, *558*, pp.288-291.
972 Lowery, C.M. and Fraass, A.J., 2019. Morphospace expansion paces taxonomic diversification after
973 end Cretaceous mass extinction. *Nature Ecology & Evolution*, *3*, pp. 900-904.
974 Mai, H., Speijer, R.P. and Schulte, P., 2003. Calcareous index nannofossils (coccoliths) of the
975 lowermost Paleocene originated in the late Maastrichtian. *Micropaleontology*, *49*, pp. [18]9-
976 195.
977 McQuoid, M.R., Godhe, A. and Nordberg, K., 2002. Viability of phytoplankton resting stages in the
978 sediments of a coastal Swedish fjord. *European Journal of Phycology*, *37*, pp. 191-201.
979 O’Dea, S.A., Gibbs, S.J., Bown, P.R., Young, J.R., Poulton, A.J., Newsam, C. and Wilson, P.A., 2014.
980 Coccolithophore calcification response to past ocean acidification and climate change.
981 *Nature Communications*, *5*, 5363.

982 Oksanen, J., et al., 20[18], vegan: Community Ecology Package, version 2.4-2, *in* R: A Language and
983 Environment for Statistical Computing: R Core Team, https://cran.r-294
984 project.org/package=vegan.
985 Okada, H. and Honjo, S., 1973. The distribution of oceanic coccolithophorids in the Pacific. *Deep Sea*
986 *Research and Oceanographic Abstracts, 20,* pp. 355-374.
987 Paasche, E., 2001. A review of the coccolithophorid *Emiliania huxleyi* (Prymnesiophyceae), with
988 particular reference to growth, coccolith formation, and calcification-photosynthesis
989 interactions. *Phycologia*, *40*, pp. 503-529.
990 Perch-Nielsen, K., 1985. Cenozoic calcareous nannofossils. In: Bolli, H.M., Saunders, J.B. and Perch-
991 Nielsen, K. eds., 1989. *Plankton Stratigraphy: Volume 1, Planktic Foraminifera, Calcareous*
992 *Nannofossils and Calpionellids (Vol. 1)*, pp. 427-554, Cambridge University Press.
993 Pospichal, J.J., 1994. Calcareous nannofossils at the KT boundary, El Kef: No evidence for stepwise,
994 gradual, or sequential extinctions. *Geology*, *22*, pp.99-102.
995 Pospichal, J.J., 1995, Cretaceous/Tertiary boundary calcareous nannofossils from Agost, Spain, *in*
996 Flores, J.A., and Sierro, F.J., eds., Proceedings of the 5th International Nannoplankton
997 Association Conference in Salamanca: Salamanca, Universidad de Salamanca Press, p. [18]5–
998 217.
999 Rhodes, M.C. and Thayer, C.W., 1991. Mass extinctions: ecological selectivity and primary
1000 production. *Geology*, *19*, pp. 877-880.
1001 Ribeiro, S., Berge, T., Lundholm, N., Andersen, T.J., Abrantes, F. and Ellegaard, M., 2011.
1002 Phytoplankton growth after a century of dormancy illuminates past resilience to catastrophic
1003 darkness. *Nature Communications*, *2, 311,* doi: https://doi.org/10.1038/ncomms1314.
1004 Schueth, J.D., 2009. *A Multivariate Analysis of the Recovery of Calcareous Nannoplankton and*
1005 *Planktonic Foraminifera from the Cretaceous/Paleogene (K/P) Mass Extinction.* (MS Thesis,
1006 The Pennsylvania State University)
1007 Schueth, J.D., Bralower, T.J., Jiang, S. and Patzkowsky, M.E., 2015. The role of regional survivor
1008 incumbency in the evolutionary recovery of calcareous nannoplankton from the
1009 Cretaceous/Paleogene (K/Pg) mass extinction. *Paleobiology*, *41*, pp.661-679.
1010 Schulte, P., Alegret, L., Arenillas, I., Arz, J.A., Barton, P.J., Bown, P.R., Bralower, T.J., Christeson, G.L.,
1011 Claeys, P., Cockell, C.S., Collins, G.S., et al. 2010. The Chicxulub asteroid impact and mass
1012 extinction at the Cretaceous-Paleogene boundary. *Science*, *327*, pp.1214-12[18].
1013 Sepkoski, J.J., 2002. A Compendium of Fossil Marine Animal Genera. *Bulletin of American*
1014 *Paleontology, 363,* pp. 1-560.
1015 Sepúlveda, J., Alegret, L., Thomas, E., Haddad, E., Cao, C. and Summons, R.E., 2019. Stable Isotope
1016 Constraints on Marine Productivity Across the Cretaceous-Paleogene Mass Extinction.
1017 *Paleoceanography and Paleoclimatology*, *34*, pp. 1195-1217.
1018 Sepúlveda, J., Wendler, J.E., Summons, R.E. and Hinrichs, K.U., 2009. Rapid resurgence of marine
1019 productivity after the Cretaceous-Paleogene mass extinction. *Science*, *326*, pp. 129-132.
1020 Sessa, J.A., Bralower, T.J., Patzkowsky, M.E., Handley, J.C. and Ivany, L.C., 2012. Environmental and
1021 biological controls on the diversity and ecology of Late Cretaceous through early Paleogene
1022 marine ecosystems in the US Gulf Coastal Plain. *Paleobiology*, *38*, pp.2[18]-239.
1023 Sheehan, P.M., Coorough, P.J., Fastovsky, D.E. and Ryder, G., 1996. Biotic selectivity during the K/T
1024 and Late Ordovician extinction events. *Geological Society of America Special Paper*, *307*,
1025 pp.477-489.
1026 Sheward, R.M., Poulton, A.J., Gibbs, S.J., Daniels, C.J. and Bown, P.R., 2017. Physiology regulates the
1027 relationship between coccosphere geometry and growth phase in coccolithophores.
1028 *Biogeosciences*, *14*, pp.1493-1509.
1029 Sibert, E., Friedman, M., Hull, P., Hunt, G. and Norris, R., 20[18]. Two pulses of morphological
1030 diversification in Pacific pelagic fishes following the Cretaceous–Palaeogene mass extinction.
1031 *Proceedings of the Royal Society B*, *285*, doi: 10.1098/rspb.20[18].1194.
1032 Sibert, E.C. and Norris, R.D., 2015. New Age of Fishes initiated by the Cretaceous− Paleogene mass
1033 extinction. *Proceedings of the National Academy of Sciences*, *112*, pp. 8537-8542.

Slimani, H., Louwye, S. and Toufiq, A., 2010. Dinoflagellate cysts from the Cretaceous–Paleogene boundary at Ouled Haddou, southeastern Rif, Morocco: biostratigraphy, paleoenvironments and paleobiogeography. *Palynology*, *34*, pp. 90-124.

Sluijs, A., Pross, J. and Brinkhuis, H., 2005. From greenhouse to icehouse; organic-walled dinoflagellate cysts as paleoenvironmental indicators in the Paleogene. *Earth-Science Reviews*, *68*, pp.281-315.

Smit, J.,1982. Extinction and evolution of planktonic foraminifera after a major impact at the Cretaceous/Tertiary boundary. *Geological Society of America Special Paper, 190,* pp. 329-352.

Soudry, D., Glenn, C.R., Nathan, Y., Segal, I. and VonderHaar, D., 2006. Evolution of Tethyan phosphogenesis along the northern edges of the Arabian–African shield during the Cretaceous–Eocene as deduced from temporal variations of Ca and Nd isotopes and rates of P accumulation. *Earth-Science Reviews*, *78*, pp. 27-57.

Tantawy, A.A.A., 2003. Calcareous nannofossil biostratigraphy and paleoecology of the Cretaceous–Tertiary transition in the central eastern desert of Egypt. *Marine Micropaleontology*, *47*, pp.323-356.

Taucher, J., Jones, J., James, A., Brzezinski, M.A., Carlson, C.A., Riebesell, U. and Passow, U., 2015. Combined effects of CO2 and temperature on carbon uptake and partitioning by the marine diatoms *Thalassiosira weissflogii* and *Dactyliosolen fragilissimus*. *Limnology and Oceanography*, *60*, pp.901-919.

Thierstein, H.R. and Berger, W.H., 1978. Injection events in ocean history. *Nature*, *276*, pp.461-466.

Thoday, J. M. and Boam, T. B. 1959., Effects of disruptive selection. II. Polymorphism and divergence without isolation. *Heredity*, *13,* pp. 205–2[18].

Thomas, E., 2007. Cenozoic mass extinctions in the deep sea: What perturbs the largest habitat on Earth? *The Geological Society of America Special Paper, 424*, pp. 1-23.

Tozzi, S., Schofield, O. and Falkowski, P., 2004. Historical climate change and ocean turbulence as selective agents for two key phytoplankton functional groups. *Marine Ecology Progress Series*, *274*, pp.123-132.

Valentine, J.W., 1969. Patterns of taxonomic and ecological structure of the shelf benthos during Phanerozoic time. *Palaeontology*, *12*, pp. 684-709.

Vellekoop, J., Esmeray-Senlet, S., Miller, K.G., Browning, J.V., Sluijs, A., van de Schootbrugge, B., Sinninghe Damsté, J.S. and Brinkhuis, H., 2016. Evidence for Cretaceous-Paleogene boundary bolide "impact winter" conditions from New Jersey, USA. *Geology*, *44*, pp.619-622.

Vellekoop, J., Sluijs, A., Smit, J., Schouten, S., Weijers, J.W., Damsté, J.S.S. and Brinkhuis, H., 2014. Rapid short-term cooling following the Chicxulub impact at the Cretaceous–Paleogene boundary. *Proceedings of the National Academy of Sciences*, *111*, pp.7537-7541.

Vellekoop, J., Smit, J., van de Schootbrugge, B., Weijers, J.W., Galeotti, S., Damste, J.S.S. and Brinkhuis, H., 2015. Palynological evidence for prolonged cooling along the Tunisian continental shelf following the K–Pg boundary impact. *Palaeogeography, Palaeoclimatology, Palaeoecology*, *426*, pp.216-228.

Vellekoop, J., Woelders, L., Açikalin, S., Smit, J., Van De Schootbrugge, B., Yilmaz, I.O., Brinkhuis, H. and Speijer, R.P., 2017. Ecological response to collapse of the biological pump following the mass extinction at the Cretaceous-Paleogene boundary. *Biogeosciences*, *14*, pp.885-900.

Vellekoop, J., Woelders, L., van Helmond, N.A., Galeotti, S., Smit, J., Slomp, C.P., Brinkhuis, H., Claeys, P. and Speijer, R.P., 20[18]. Shelf hypoxia in response to global warming after the Cretaceous-Paleogene boundary impact. *Geology*, *46*, pp.683-686.

Vermeij, G.J., 1977. The Mesozoic marine revolution: evidence from snails, predators and grazers. *Paleobiology*, *3*, pp. 245-258.

Whittle, R.J., Witts, J.D., Bowman, V.C., Crame, J.A., Francis, J.E. and Ineson, J., 2019. Nature and timing of biotic recovery in Antarctic benthic marine ecosystems following the Cretaceous–Palaeogene mass extinction. *Palaeontology*, *62*, pp. 919-934.

Witts, J.D., Whittle, R.J., Wignall, P.B., Crame, J.A., Francis, J.E., Newton, R.J. and Bowman, V.C., 2016. Macrofossil evidence for a rapid and severe Cretaceous–Paleogene mass extinction in Antarctica. *Nature Communications*, *7*, 11738.

Figures

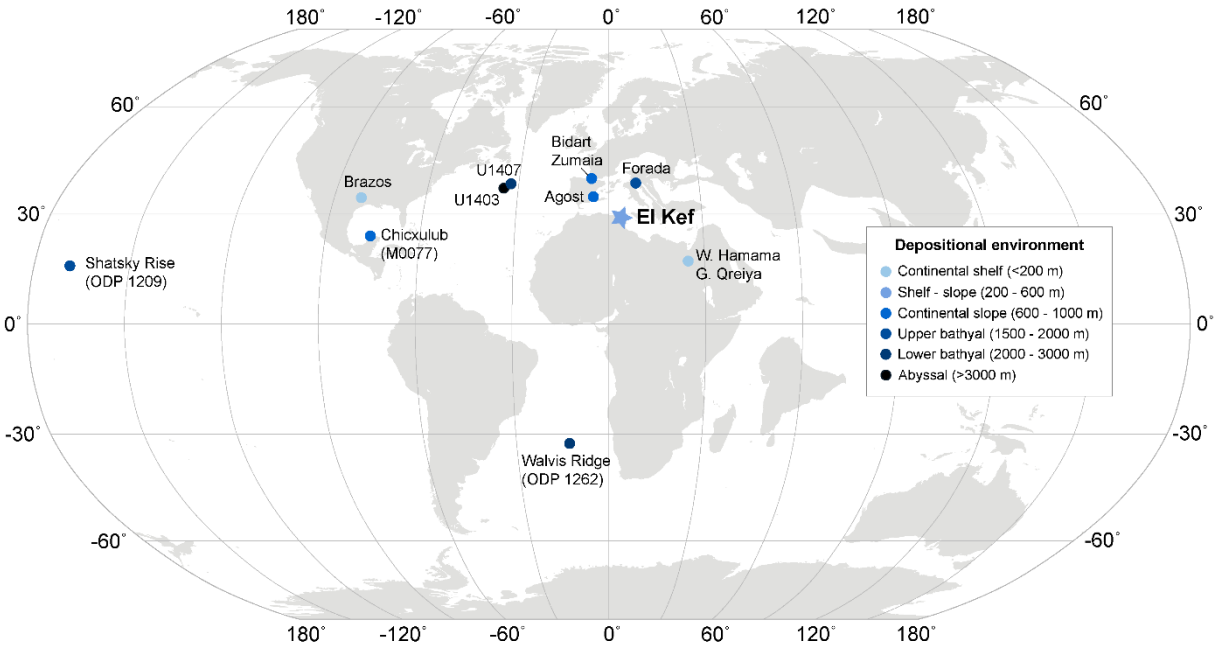

Fig. 1: Paleogeographic map of the Paleocene showing the location of El Kef, Tunisia in relation to the other K-Pg sites used for comparison.

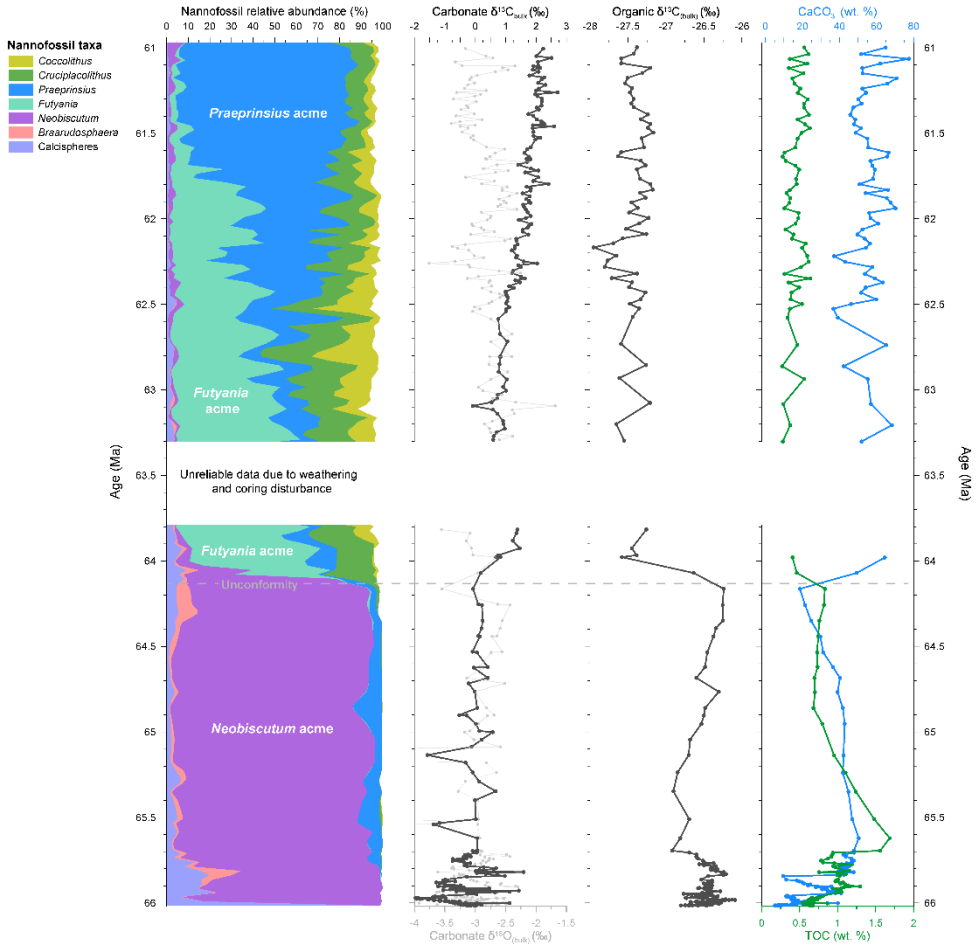

Fig. 2: A: Graph showing changes in the relative abundance of different calcareous nannoplankton taxa with time at El Kef (Tunisia). B: Bulk carbonate $\delta^{13}C$ and $\delta^{13}C$ record. C: Bulk organic $\delta^{13}C$ record D: % TOC and % CaCO3.

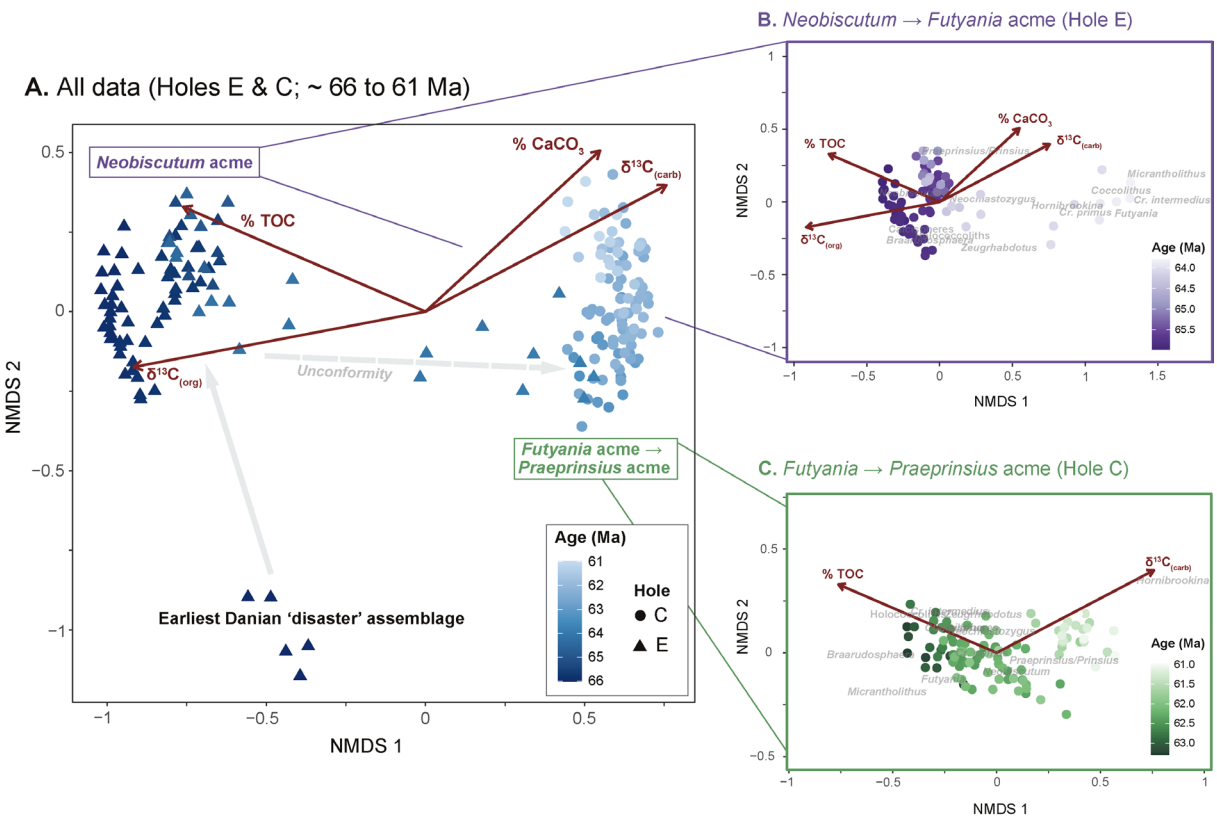

Fig. 3: Nonmetric multidimensional scaling (NMDS) ordination plots showing the variation between samples at El Kef. A: Variation between samples in El Kef Holes E and C. B: Variation between samples in El Kef E. C: Variation between samples in El Kef C. Sample scores are colored by age, with darker shades representing older samples. The red vectors on each ordination show the regression of various external variables against the NMDS scores, allowing us to determine which parameters were most important in driving changes in nannoplankton community composition. The length of each of the vectors correspond to the strength of each of these correlations, with bolded vectors representing statistically significant relationships.

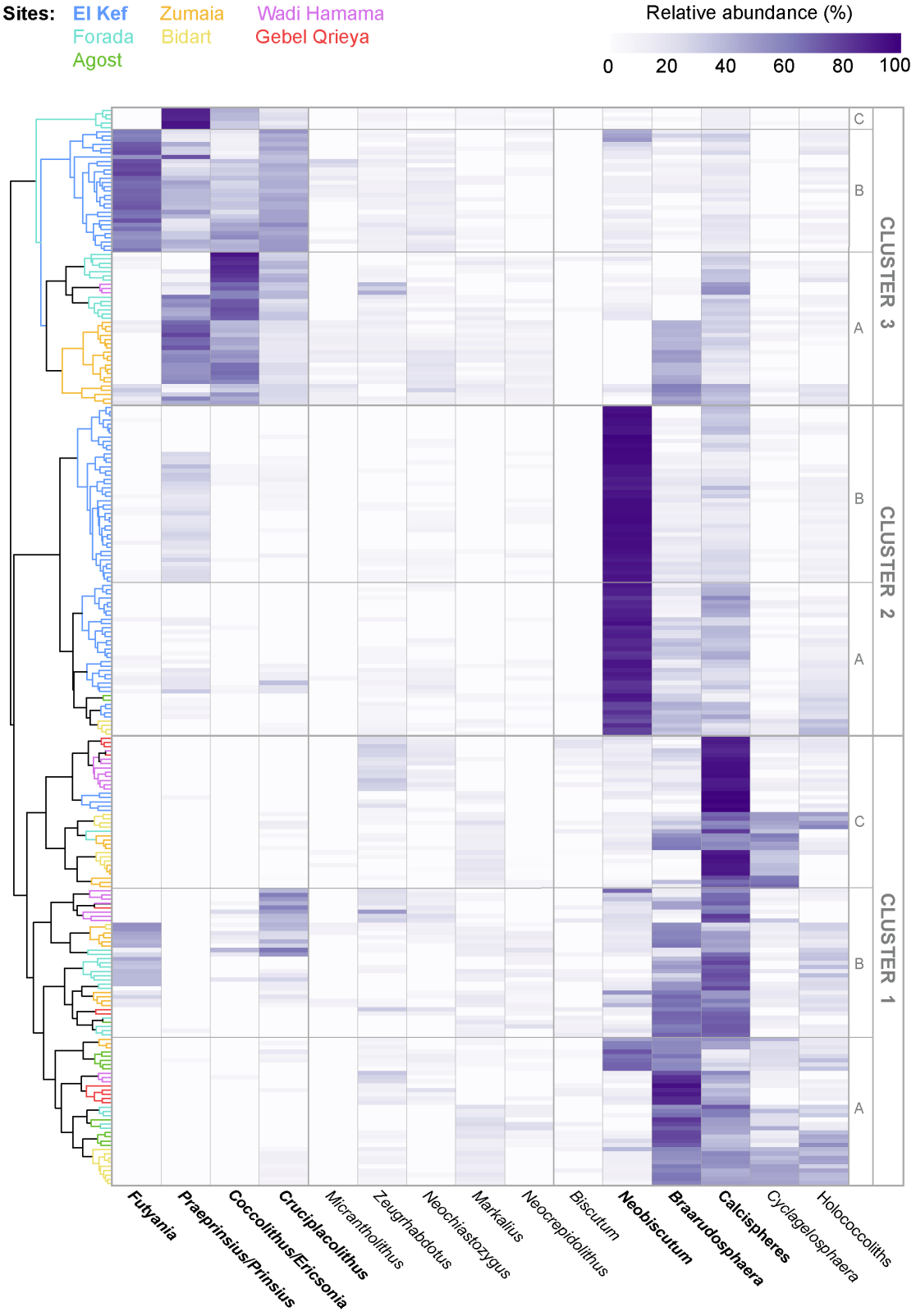

Fig. 4: Two-way cluster analysis showing the differences in nannoplankton community composition within the paleo-Tethys. The sites used are: El Kef, Tunisia (this study; blue); Forada, Italy (from Fornaciari et al. 2007; teal); Agost, Spain (from Pospichal, 1994; green); Zumaia, Spain (from Jiang et al. 2019; orange); Bidart, France (Jiang et al. 2019; yellow); Wadi Hamama, Egypt (from Tantawy, 2003; pink); and Gebel Qreiya, Egypt (Tantawy, 2003; red). Taxon names are displayed on the horizonatal axis and the samples along the vertical axis are colored according to site. The purple

colors within the grid are related to the dominance of each taxa, with darker shades corresponding to a relatively high abundance of that taxon.

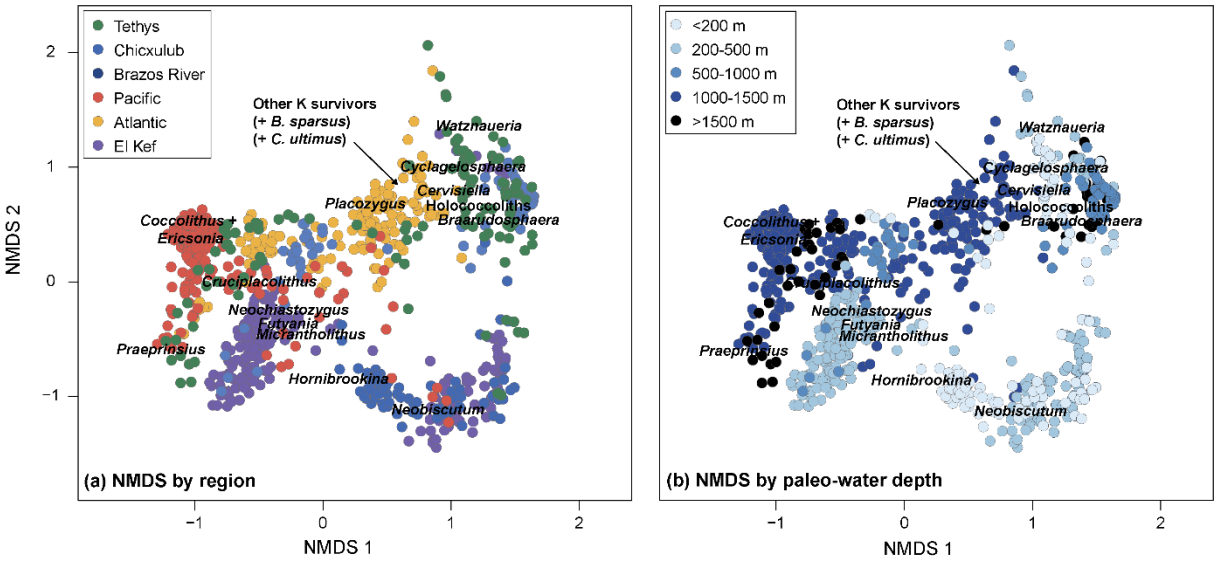

Fig. 5: NMDS ordinations comparing changes in nannoplankton community composition at El Kef to a global K-Pg dataset. The sites used sample a diverse range of geographical regions and paleoenvironments. A: NMDS sample scores colored by geographical region. B: NMDS sample scores colored by interpreted paleodepth.

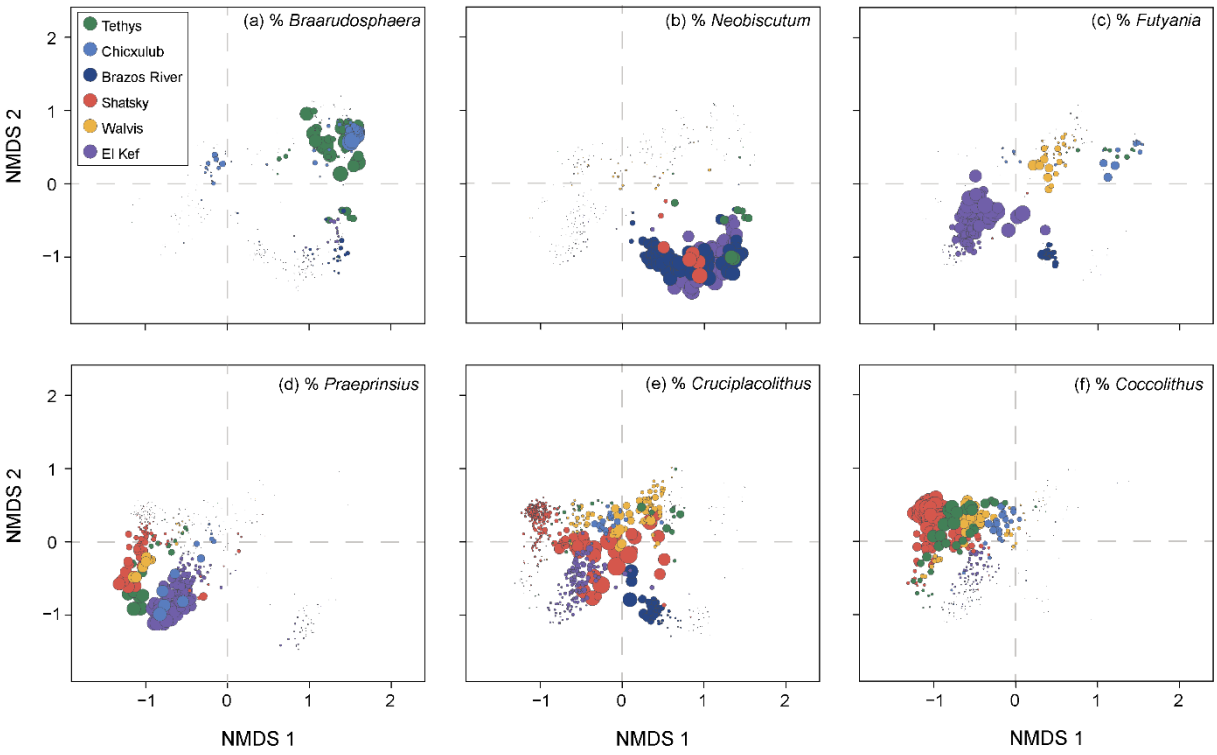

Fig. 6: Global NMDS scores colored by geographic region. The size of each point is scaled in proportion to the relative abundance of a specific genus within a sample. These genera are: A: *Braarudosphaera*. B: *Neobiscutum*. C: *Futyania.* D: *Praeprinsius*. E: *Cruciplacolithus*. F: *Coccolithus*.